# CHAPTER IV

RESULTS AND DISCUSSIONS

4.1   Synthesis of p-chloromethylstyrene

This section was involved the synthesis of vinyl benzyl chloride monomer by chloromethylation of 2-bromoethyl benzene and then dehydrobromination using the method of Kondo et al [39]. It was understanding that this was the most suitable method due to chemical safety, reactant availability and high product yield.

4.1.1   Chloromethylation of 2-bromoethyl benzene

The principal value of chloromethylation lies in the ease of displacement of the benzylic chloride by nucleophiles. The chloromethyl group, $-CH_2Cl$, can be introduced into aromatic compounds by treatment with formaldehyde and hydrogen chloride in the presence of the lewis acid, $ZnCl_2$. By passing hydrogen chloride into a suspension of paraformaldehyde and zinc chloride in carbondisulfide ; the acid firstly liberates formaldehyde from paraformaldehyde and then takes part in the condensation.
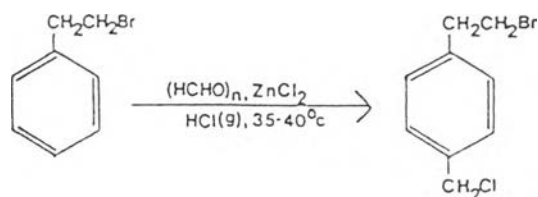
Scheme 4.1

Hydrochloric gas was generated, when concentrated hydrochloric acid was dropped to concentrated sulfuric acid, and the gas then passed through the solution of 2-phenylethyl bromide in carbon disulfide. It was purged for 30 min. And then the first portion of anhydrous zinc chloride and paraformaldehyde was mixed with. The solution became clear when the hydrochloric gas was purged at the interval time. Then, the second and third portion were mixed with the solution in the same manner. Until the reaction was completed, the light yellow viscous liquid was obtained.

The proposed mechanism of this reaction was revealed in Scheme 4.3 [40,41]. The electrophilic entity was the hydroxymethyl cation, which would react with chloride ion to give an alcoholic product, then was converted into the chloromethyl product in the presence of hydrogen chloride.
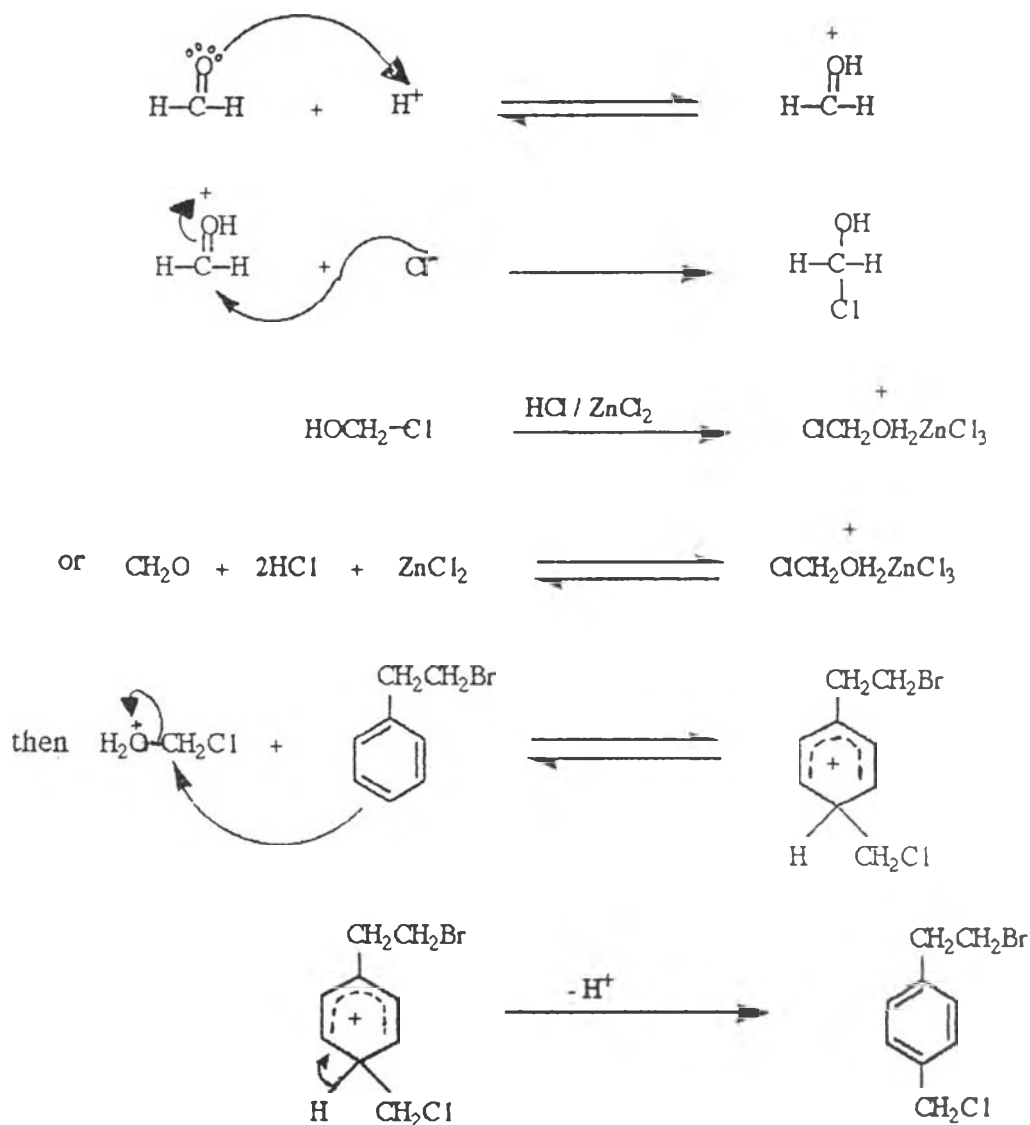
Scheme 4.2

The resulting mixture was extracted with dilute solution of sodium carbonate to remove remaining hydrochloric acid. Followed with double distilled water the basic solution was removed from the mixture. The mixture was vacuum distilled to get o- and p-(2-bromoethyl) benzyl

chloride. The unreacted reactants in residue, 2-phenylethyl bromide, was reused. Petroleum ether was used as precipitating solvent by adding to the frozen mixture of o- and p-(2-bromoethyl) benzyl chloride. Accordingly, o-(2-bromoethyl) benzyl chloride was dissolved in petroleum ether, it could be decanted. The p-(2-bromoethyl) benzyl chloride crystal was recrystallized until insignificant amount of o-(2-bromoethyl) benzyl chloride was observed.

When p-(2-bromoethyl) benzyl chloride was recrystallized for several times, the resulting crystal was clearly long needle-like materials. It should be noted that the crystal was dissolved instantly in petroleum ether and became the crystal product at room temperature, after repeated recrystallization. The p-(2-bromoethyl) benzyl chloride had the melting point 50°-52^OC, with 46% yield.

The infrared spectrum (Figure 4.1) of p-(2-bromoethyl) benzyl chloride exhibited the characteristic absorption peaks at 850 cm^{-1} and 1260 cm^{-1}. They were assigned to =C-H out of plane bending of para-disubstituted benzene and to C-Cl bending, respectively. The C-Cl stretching appeared at the absorption frequency 670 cm^{-1}. Other assignments were summarized in Table 4.1.
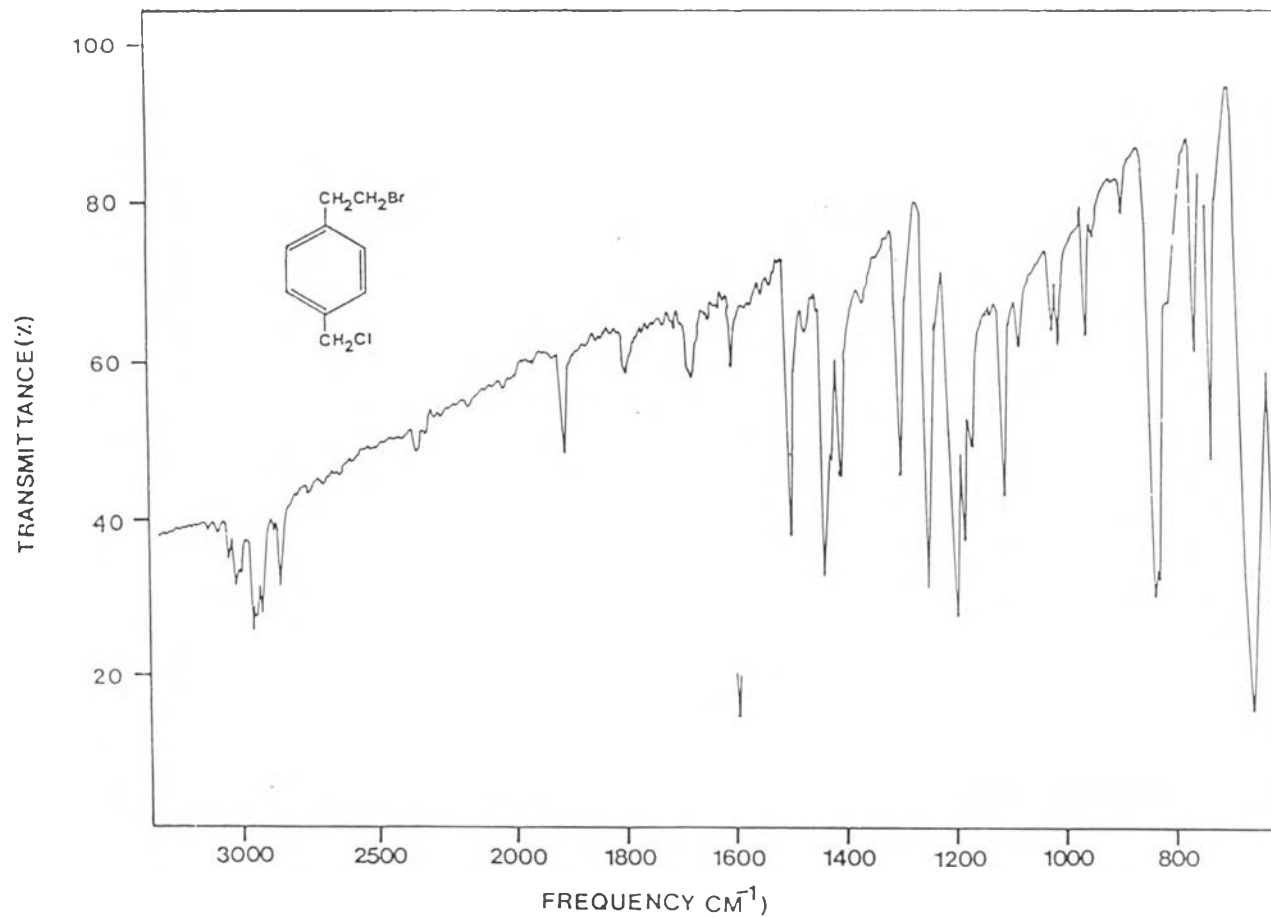
Figure 4.1 The IR spectrum (KBr) of p-(2-bromoethyl) benzyl chloride

Table **4.1** The assignment for the IR spectrum of p-(2-bromoethyl) benzyl chloride

Absorption frequency (cm^{-1})	Tentative assignment
3030	C-H aromatic str.
2970	C-H aliphatic str.
1920,1805,1690	overtone region of aromatic ring (p-disubstituted aromatic)
1510,1450,1420	C=C stretching
1260	C-Cl bending ($-CH_2-Cl$)
1210	C-Br bending ($-CH_2-Br$)
850	=C-H out of plane bending (p-disubtituted aromatic)
670	C-Cl str.
620	C-Br str.

The proton NMR (Figure 4.2) of p-(2-bromoethyl) benzyl chloride exhibited the characteristic singlet signal at 4.53 ppm due to two protons of chloromethyl group and the doublet signal of para-disubstituted aromatic ring was shown at 7.18 and 7.28 ppm. Other assignments were summarized in Table 4.2.
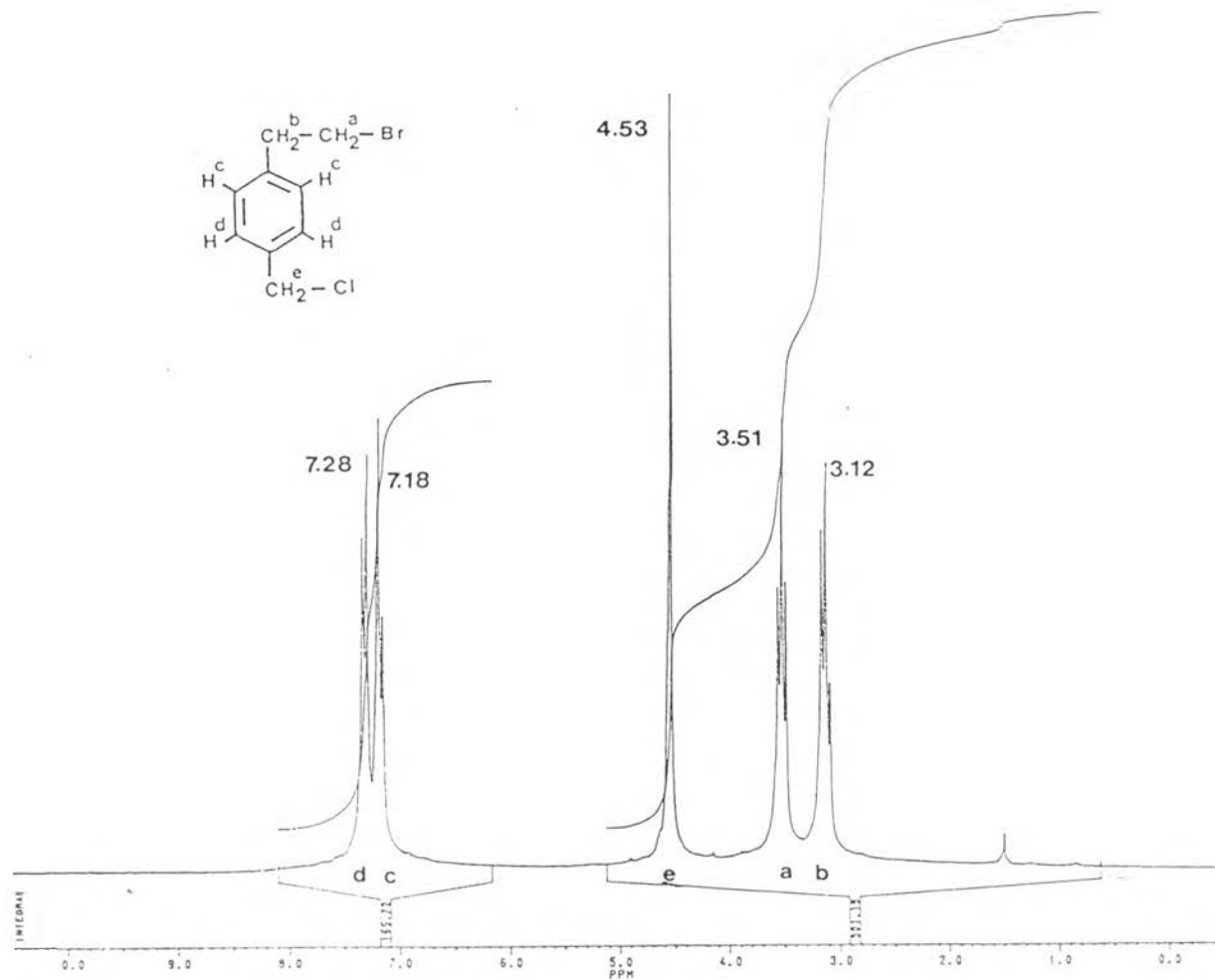
Figure 4.2 The ^{1}H-NMR spectrum (CDCl$_3$) of p-(2-bromoethyl) benzyl chloride

Table 4.2 The assignment for the ^{1}H-NMR spectrum of

p-(2-bromoethyl) benzyl chloride

Chemical shift (ppm)	Multiplicity	Tentative assignment
7.28	d, 2H (J=7.94 Hz)	H^d (aromatic ring)
7.18	d, 2H (J=7.96 Hz)	H^c (aromatic ring)
4.53	s, 2H	-CH$_2$-Cl
3.51	t, 2H (J=7.46 Hz)	-CH$_2$-Br
3.12	t, 2H (J=7.39 Hz)	-CH$_2$-

The carbon NMR (Figure 4.3) of p-(2-bromoethyl) benzyl chloride exhibited the important carbon signal of chloromethyl group at 45.89 ppm and the aromatic ring signals were at 139.06, 136.06, 129.95 and 128.77 ppm which corresponded to p-disubstituted aromatic compound. Other assignments were summarized in Table 4.3.
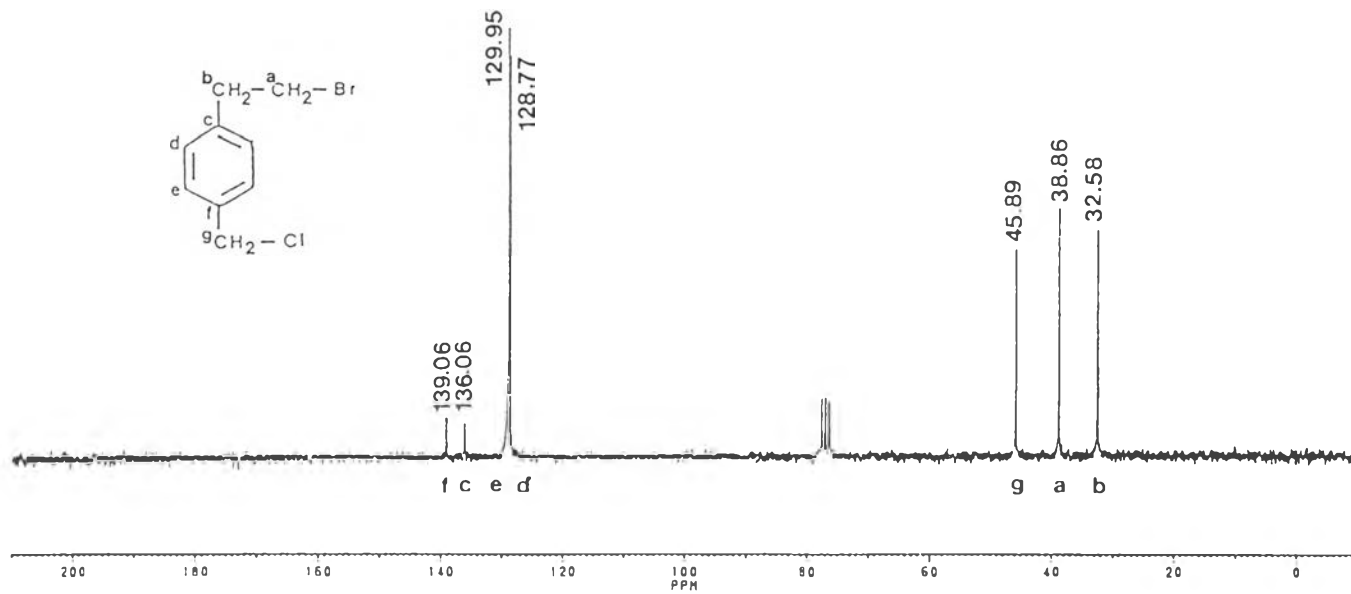
Figure 4.3 The ^{13}C-NMR spectrum (CDCl$_3$) of p-(2-bromoethyl) benzyl chloride

Table 4.3 The assignment for the ^{13}C-NMR spectrum of

p-(2-bromoethyl) benzyl chloride

Chemical shift (ppm)	Tentative assignment
139.06	$-^f C=$ (aromatic ring)
136.06	$-^c C=$ (aromatic ring)
129.95	$-^e C=$ (aromatic ring)
128.77	$-^d C=$ (aromatic ring)
45.89	$-^g CH_2-Cl$
38.86	$-^a CH_2-Br$
32.58	$-^b CH_2-$

The mass spectrum (Figure 4.4) of p-(2-bromoethyl) benzyl chloride exhibited the molecular ion (M^+) at m/e 232 and the base peak at m/e 117 which was the fragmentation by the loss of Cl radical and HBr molecule. Other assignments were summarized in Table 4.4. The mass fragmentation pattern was summarized in scheme 4.3.
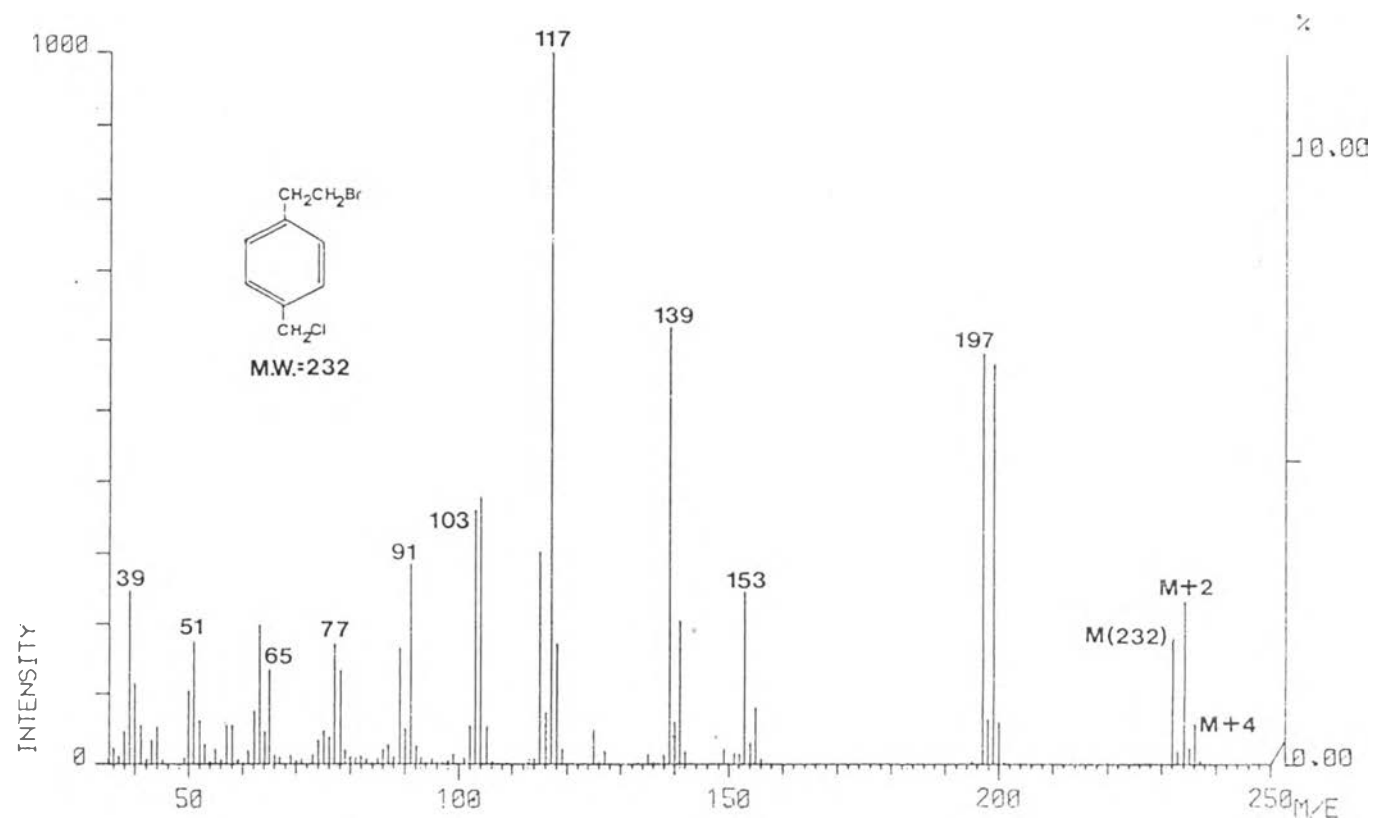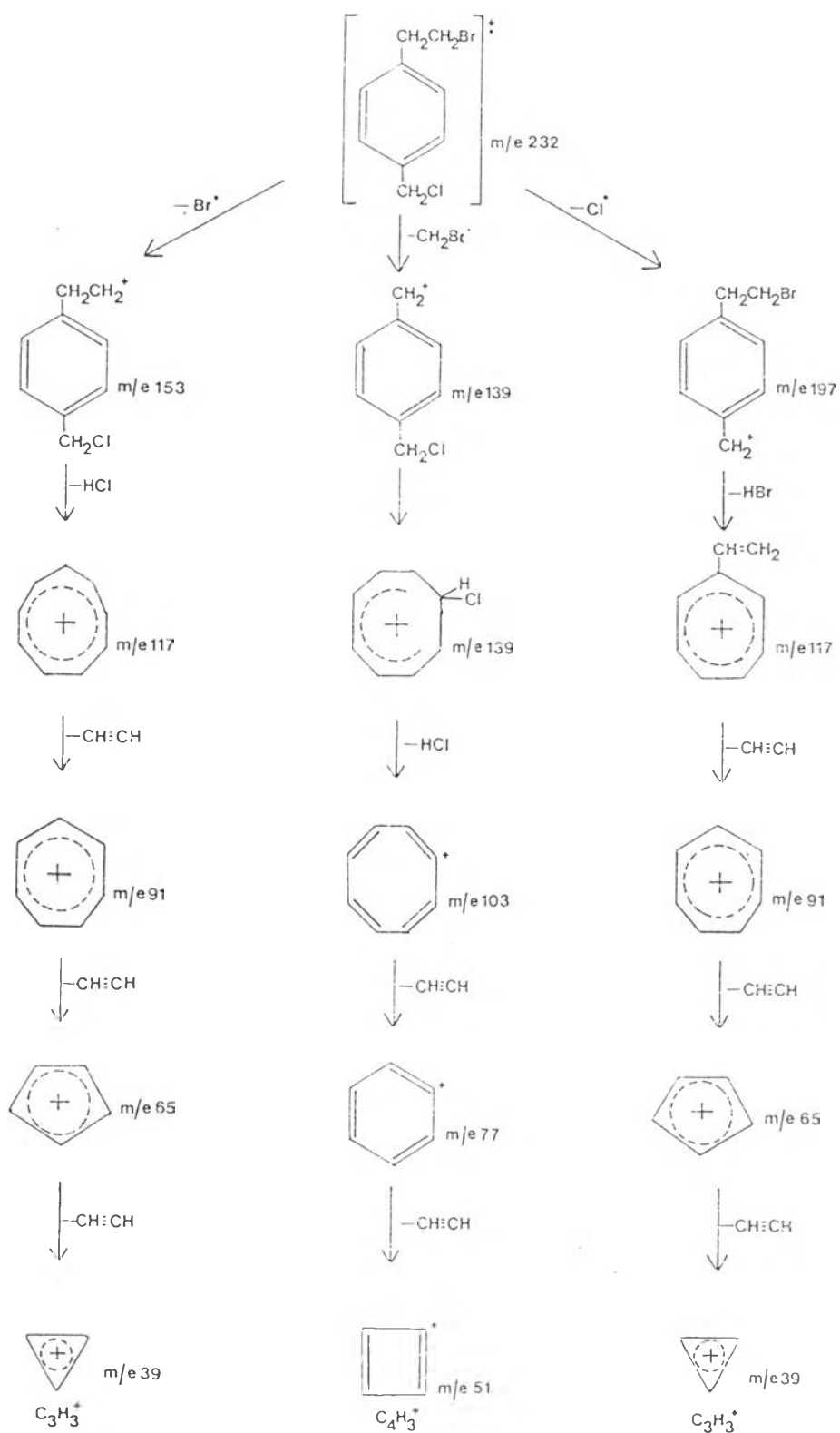
Figure 4.4 The mass spectrum of p-(2-bromoethyl) benzyl chloride

Table 4.4 The assignment for the mass spectrum of p-chloromethyl styrene

| m/e	Raw intensity	Relative intensity
39.0	134.5	247.6
51.0	96.9	178.4
65.0	72.8	134.0
77.0	93.5	172.1
91.0	155.0	285.3
103.0	196.4	361.5
117.0	543.2	1000.0
139.0	337.7	621.6
153.0	133.8	246.3
197.0	317.9	585.2
199.0	308.1	567.2
232.0	97.4	179.3
234.0	126.3	232.6
236.0	31.2	57.4

Scheme 4.3

From the spectroscopic data it could be concluded that the chloromethylation of 2-phenylethyl bromide by using paraformaldehyde and hydrogen chloride in the presence of zinc chloride anhydrous afforded p-(2-bromoethyl) benzyl chloride as a white needle-crystal product with the percentage yield of forty-six.

4.1.2 Dehydrobromination of p-(2-bromoethyl) benzyl chloride

The vinyl benzyl chloride was prepared by simply heating together the p-(2-bromoethyl) benzyl chloride and a basic solution of potassium-tert-butoxide dissolved in tert-butyl alcohol. The reaction equation could be revealed as below.
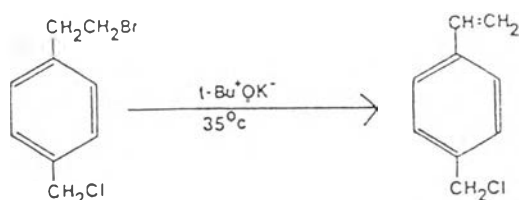
Scheme 4.4

Dehydrobromination involved the removal of the bromine atom together with a hydrogen atom from a carbon adjacent to the one bearing the bromine. So the reagent required for the elimination of what amounts to a molecule of acid was a strong base. The mechanism of dehydrobromination of p-(2-bromoethyl)benzyl chloride was shown as following.
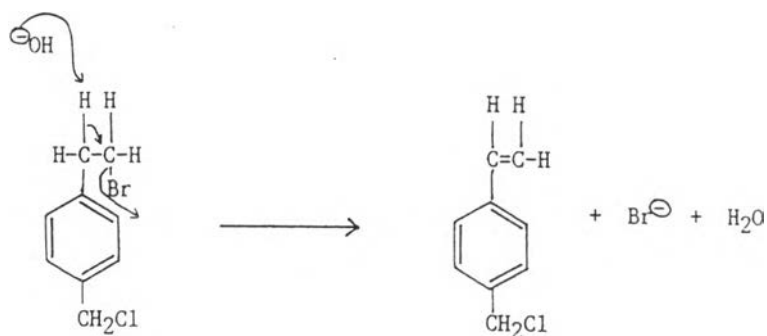
Scheme 4.5

The infrared spectrum (Figure 4.5) of vinyl benzyl chloride exhibited the characteristic absorption peaks at 660 cm^{-1} assigned to C-Cl stretching, at 820 cm^{-1} assigned to =C-H out of plane bending of aromatic (para-disubstitued aromatic) and at 1380 cm^{-1} assigned to =CH$_2$ in-place bending of alkene. Other assignments were concluded in Table 4.5.
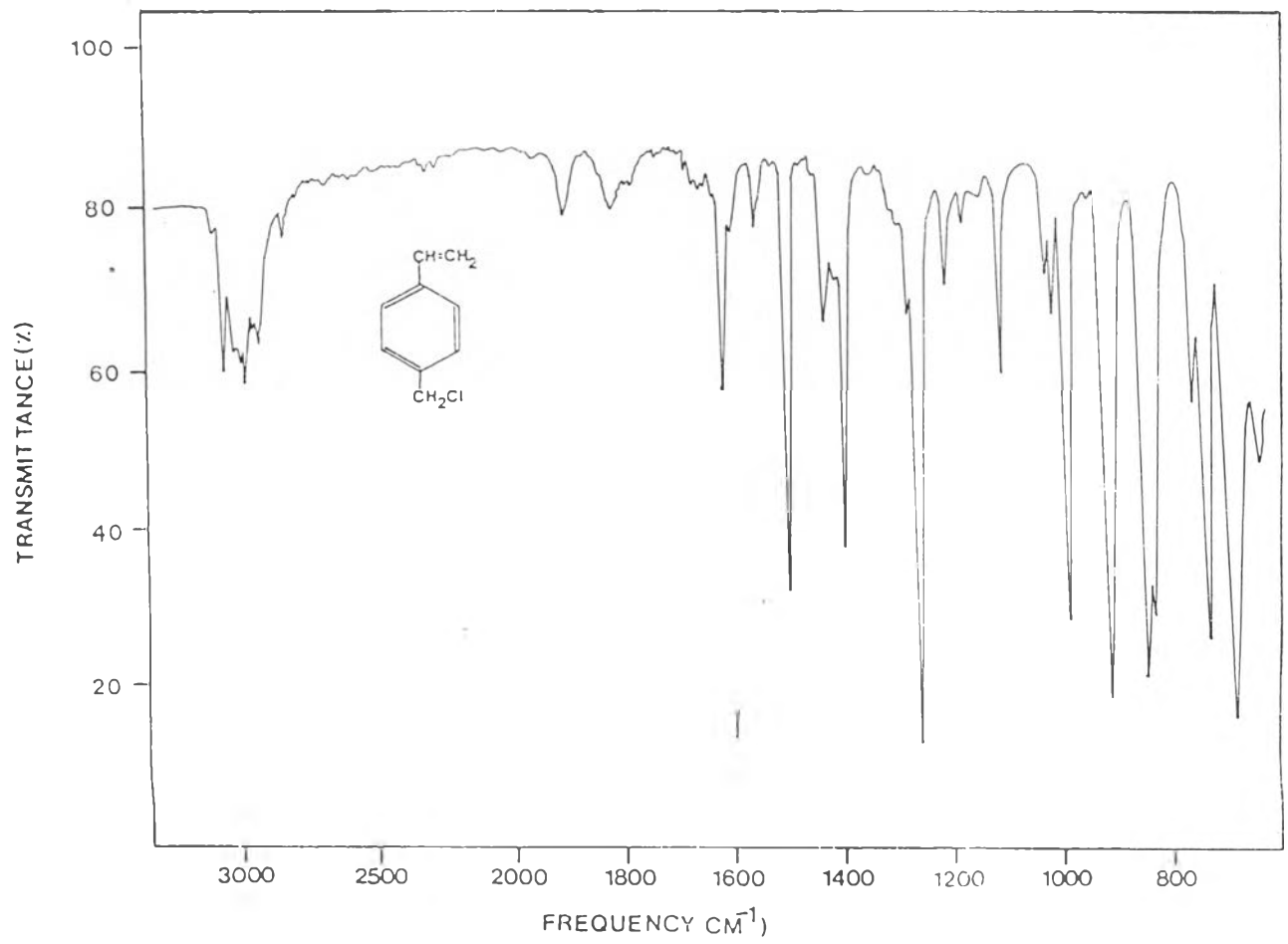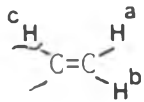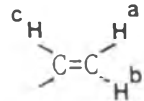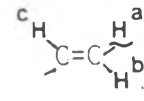
Figure 4.5 The IR spectrum (NaCl) of p-chloromethyl styrene

Table 4.5 The assignment for the IR spectrum of p-chloromethyl
styrene

Absorption frequency (cm^{-1})	Tentative assignment
3070	C-H aromatic str.
3000	C-H aliphatic str.
2940	$-CH_2-$ asym. str.
2860	$-CH_2-$ sym. str.
1905,1820	overtone region of aromatic ring (p-disubstituted aromatic)
1620	C=C vinyl str.
1500	C=C aromatic str.
1255	C-Cl bending ($-CH_2-Cl$)
1395	$=CH_2$ in-place bending of alkene
980,905	=C-H out of plane bending of alkene
835	=C-H out of plane bending of aromatic (para-disubstituted aromatic)
675	C-Cl str.

The proton NMR (Figure 4.6) of p-chloromethyl styrene exhibited the tentative assignment that there was the olefinic moiety in the molecule and corresponded to the pattern of the one reported by Kondo et al. [39] Other assignments were concluded in Table 4.6.

Table 4.6 The assignment for the ^{1}H-NMR spectrum of p-chloromethyl styrene

Chemical shift (ppm)	Multiplicity	Tentative assignment
7.46	d, 2H (8.28 Hz)	H^e (aromatic ring)
7.42	d, 2H (8.22 Hz)	H^d (aromatic ring)
6.81	d.d, 1H	
5.94	d.d, 1H	
5.39	d.d, 1H	
4.62	s, 2H	$-CH_2-Cl$

The carbon NMR (Figure 4.7) of p-chloromethyl styrene exhibited seven chemically distinct types of the carbon. Other assignments were shown in Table 4.7.
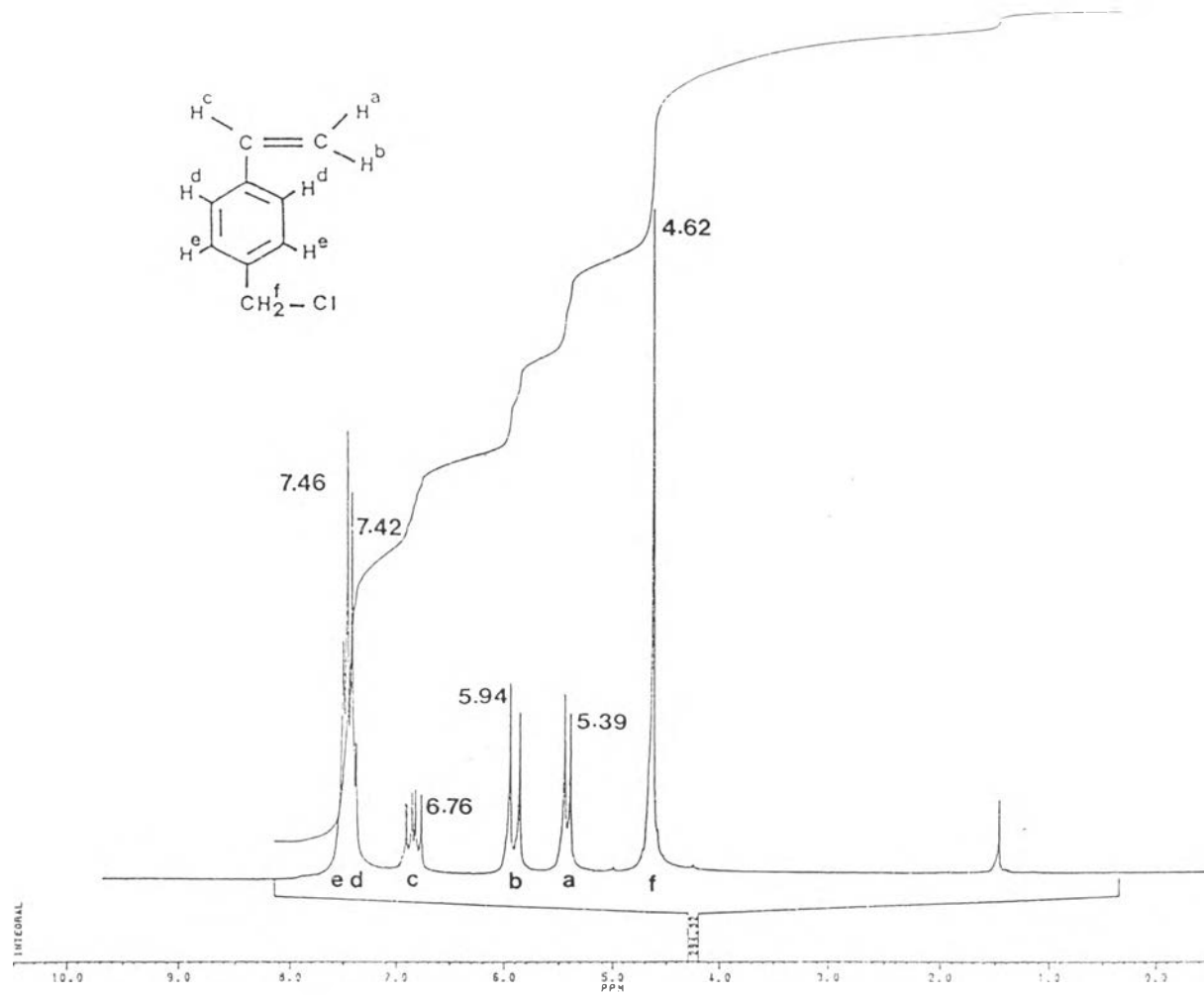
Figure 4.6 The ^{1}H-NMR spectrum (CDCl$_3$) of p-chloromethyl styrene
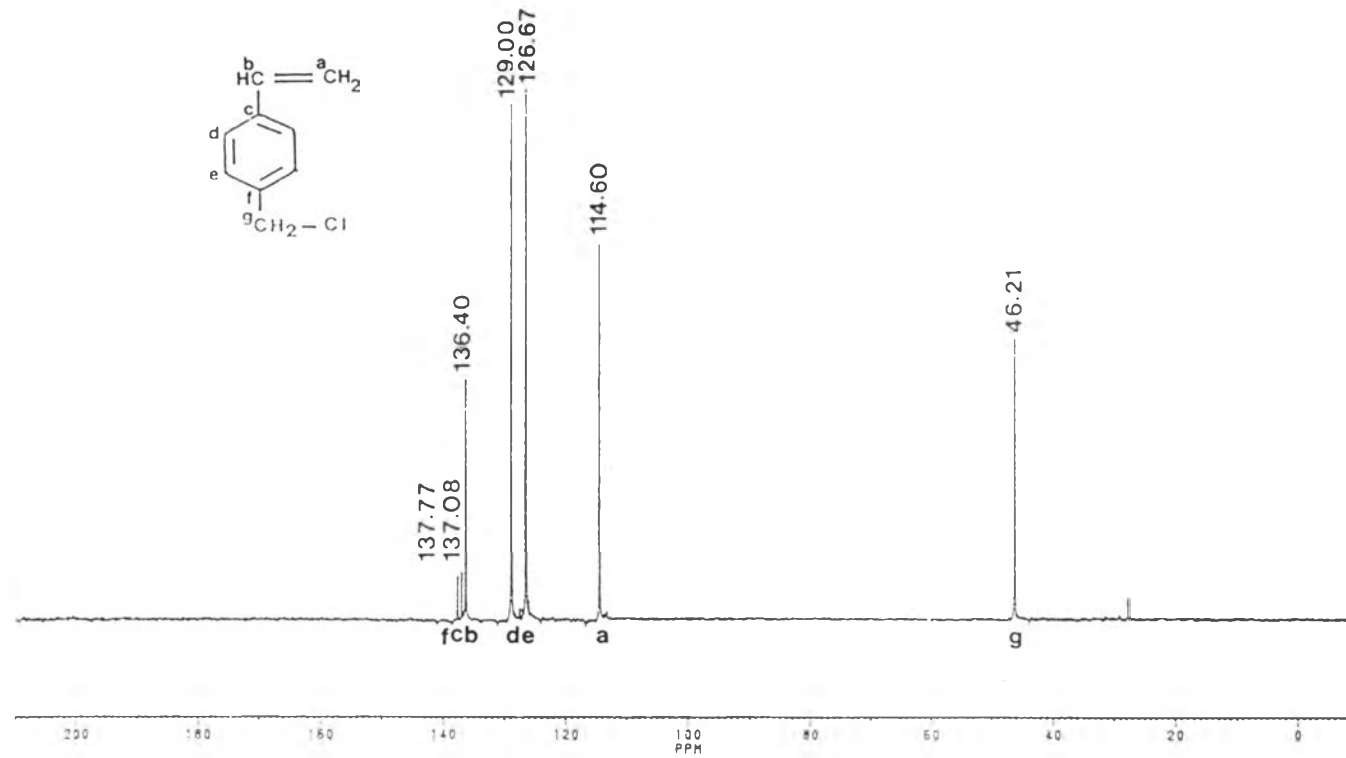
Figure 4.7 The ^{13}C-NMR spectrum (CDCl$_3$) of p-chloromethyl styrene

Table 4.7 The assignment for the ^{13}C-NMR spectrum of

p-chloromethyl styrene

Chemical shift (ppm)	Tentative assignment
137.77	$-^f$CH= (aromatic ring)
137.08	$-^c$C= (aromatic ring)
136.40	$-^b$C=
129.00	$-^d$C= (aromatic ring)
126.67	$-^e$C= (aromatic ring)
114.60	$-^a$CH$_2$-Cl
46.21	$=^g$CH$_2$

Accordingly, dehydrobromination of p-(2-bromoethyl) benzyl chloride afforded vinylbenzyl chloride monomer as viscous colorless liquid with the percentage yield of eighty-five.

4.2 Crosslinked polymers by suspension polymerization

In this part, three criteria were considered. Firstly, the formation of polymeric beads was explained. Secondly, the solvents were used for the study of polymeric bead formation. These solvents were methylisobutyl carbinol, isooctane, butanol, cyclohexanol, cyclohexanone and toluene. Finally, the solvent was chosen for the preparation of polymeric support with 3, 10 and 20 % DVB.

4.2.1 The formation of the polymeric beads

In this polymerization, the aqueous phase composed of poly(vinyl pyrrolidone), gelatin, sodium hydroxide and boric acid which should be softly mixed in order to prevent foam forming. Styrene monomer, divinyl benzene monomer, vinylbenzyl chloride monomer and benzoyl peroxide in the organic phase should also be mixed well before adding into the aqueous phase. The well preparation of both aqueous and organic phase was the important point for obtaining the spherical beads.

Poly(vinyl pyrrolidone), suspension stabilizer, and gelatin, a suspension costabilizer, were added in order to hinder the coalescence of monomer droplets and sticking together of the beads during the course of polymerization. Sodium hydroxide and boric acid were also present in order to adjust the pH of the suspension mixture which was acquired to be about 8. This was

necessary because it was the isoelectric point of gelatin, otherwise, serious impairment of the bead forming would occur.

Reproducibility of this polymerization was obtained. It was observed that poly(vinyl pyrrolidone) and gelatin affected on the formation of the polymeric beads. If the amounts of poly(vinyl pyrrolidone) and gelatin were not suitable for this polymerization, the organic phase would become sticky yellowish solution when the polymerization was completed. This events could be explained that both reagents acted as suspension stabilizer to stabilize the charge around the polymeric beads and should be used with optimum content as shown in Table 3.1. The boric acid and sodium hydroxide had the effect on the shape of polymeric beads. The non-spherical shape of the polymeric beads would form when the proportion of both reagents was not suitable.

The typical FT-IR spectrum (Figure 4.8) of poly (styrene -co- divinyl benzene -co- vinyl benzyl chloride) exhibited the characteristic absortion peaks as assignments shown in Table 4.8. The polymer did not show bands at 900-990 cm^{-1}, the range in which a terminal double bond absorbed, instead they absorbed at 2921 cm^{-1}, which indicated the formation of aliphatic methylene groups due to polymerization.
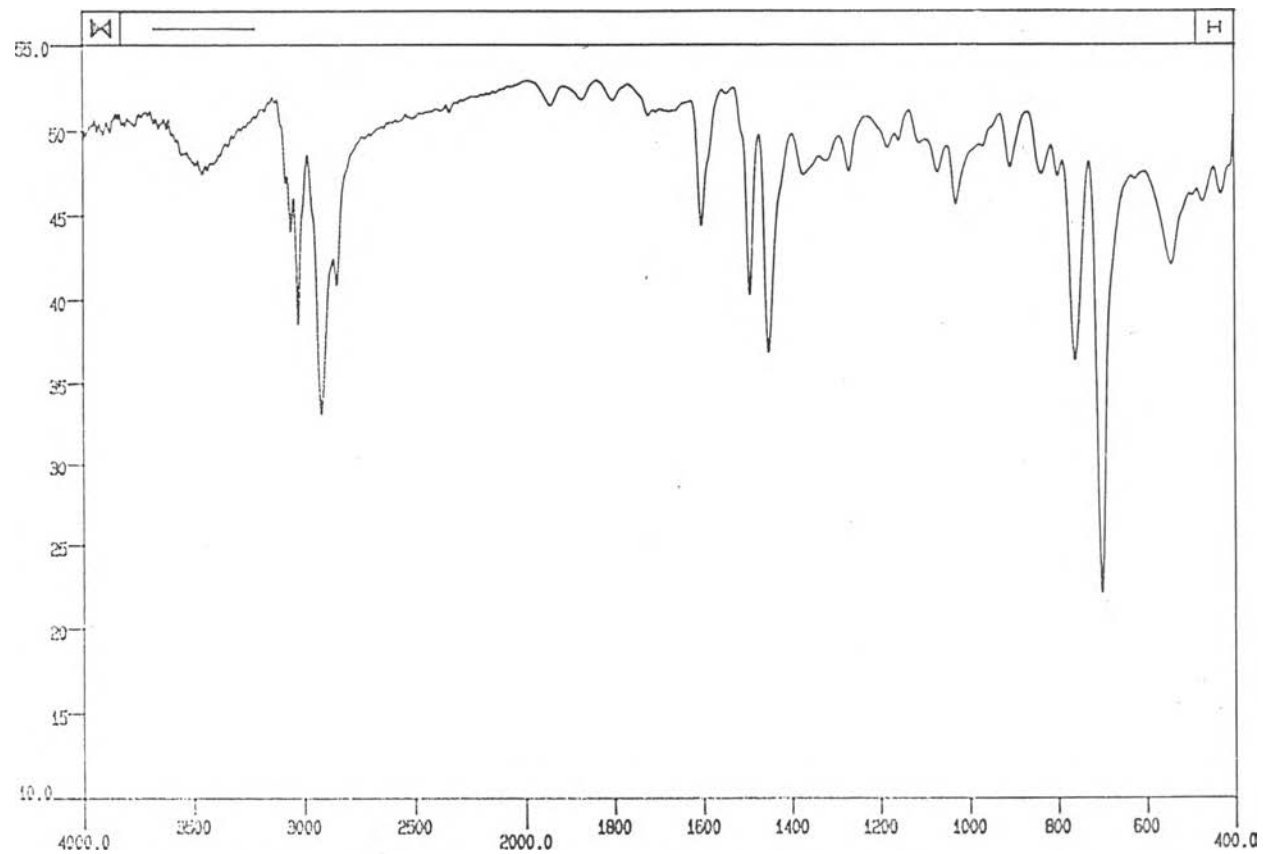
Figure 4.8 The typical FT-IR spectrum (KBr) of poly(styrene-co-divinyl benzene-co-vinylbenzyl chloride) with 10% DVB

Table 4.8 The assignment for the typical FT-IR spectrum of

poly(styrene-co-divinyl benzene-co-vinyl

benzyl chloride).

Absorption frequency (cm^{-1})	Tentative assignment of 10 % of DVB
3024	C-H aromatic str.
2921	C-H aliphatic str.
1601,1492,1450	C=C aromatic str.
1267	C-Cl bending
699	C-Cl str.

4.2.2 Effect of solvent on the formation of crosslinked polymers
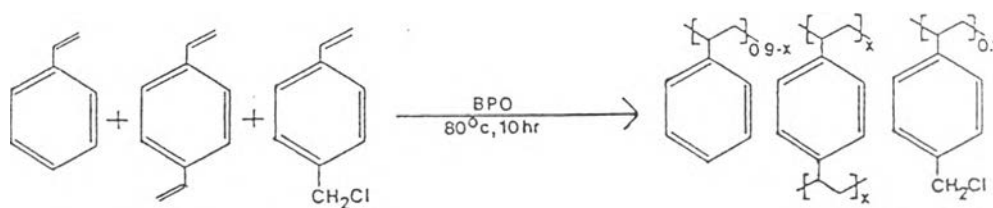
x : 0.03, 0.10 and 0.20

Scheme 4.6

In this reaction, styrene monomer, divinyl benzene monomer, vinyl benzyl chloride monomer, poly(vinyl pyrrolidone), gelatin and benzoyl peroxide were present in a homogeneous solution. Upon heating, the benzoyl peroxide decomposed and the free radical reacted with solutes, three monomers, to form oligomeric radicals. At a critical chain length, the oligomers precipitated and adsorbed poly(vinyl pyrrolidone) and gelatin to form stable particle nuclei. Once particles had been formed, they absorbed monomer from the continuous phase. From this stage on, polymerization mainly took place within the monomer-swollen particles all of the monomer was consumed [40].

The solvent was varied in both type and content. Its content was expressed as weight percentage of the total mixture of monomer and solvent. The efficiency of polymeric bead depends mainly on their porous structure. This structure was developed by using various solvents for the monomers. The extraction of the solvent from this structure caused the pore formation. The percent yield of the polymeric products were revealed in Table 4.9.

Table 4.9 Effect of solvent on the yield of poly(styrene-co-

     divinyl benzene-co-vinylbenzyl chloride) with 10% DVB.

Solvent Type	Yield (%)	Solvent Type	Yield (%)
MIBC(40%)	90.5	BU(50%)	89.1
MIBC(50%)	90.6	CY(50%)	89.2
MIBC(60%)	90.6	CN(50%)	89.1
ISO(50%)	89.7	TO(50%)	89.1

From the scanning electron microscope, it revealed that the perfectly spherical beads of poly(styrene -co- divinyl benzene -co- vinylbenzyl chloride) were obtained in all types of solvents used, except toluene (Figure 4.9). Since poly(styrene -co- divinyl benzene -co- vinylbenzyl chloride) had an aromatic moiety in the chain of the molecule, this may cause the better solubility in toluene than in other solvents. During formation of the polymeric beads, the solvent separated from the polymer which might be viewed that the solvent extruded from inside the beads to the outer region. In concomitantly with the extrusion, the solubility would occur in the same direction. Consequently, the longitudinal direction of the void formation was corresponded to the appearance of non-spherical beads.
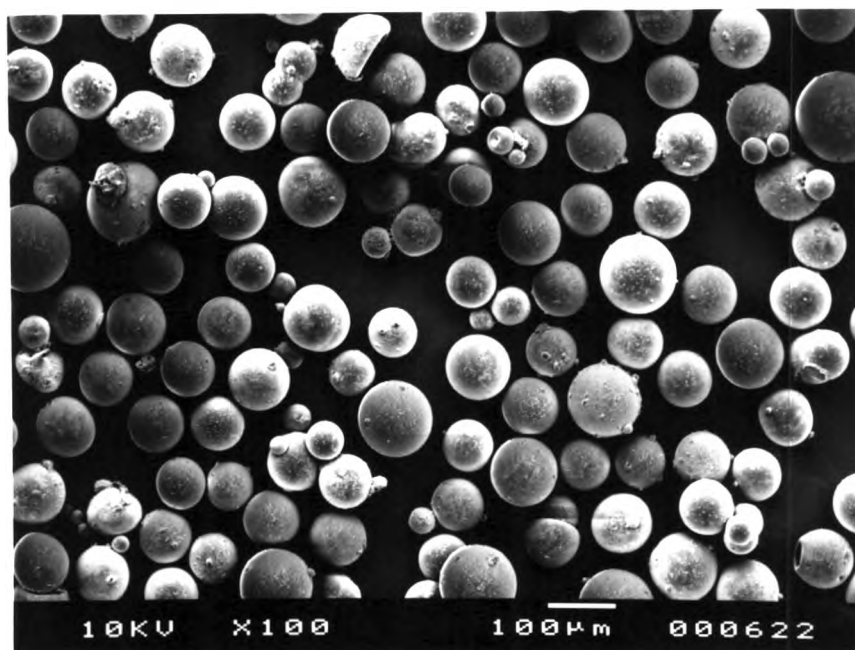
(a) Isooctane used as solvent
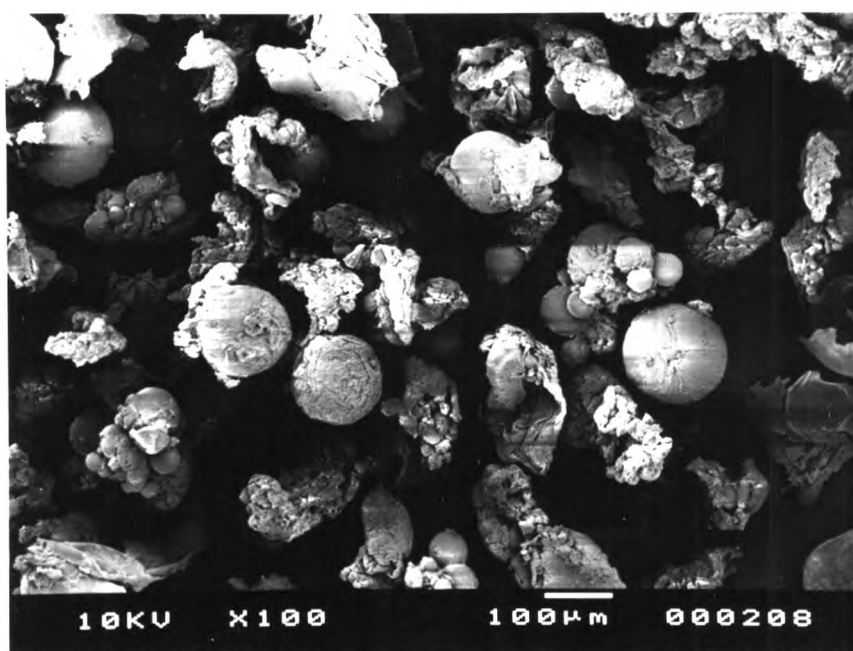
(b) Toluene used as solvent

Figure 4.9   Scanning electron micrographs of poly(styrene-co-
divinyl benzene -co- vinylbenzyl chloride) with
10% DVB, magnification with 100 times :(a) Isooctane
used as solvent, (b) Toluene used as solvent

Similar observation was reported by H.Ihara and his workers [41]. They had prepared poly(gamma-methyl-L-glutamate) using various solvents for macroreticulating by the suspension polymerization. The morphologies of the beads obtained were remarkably dependent on the chemical structure of a solvent. This was also explained by the relationship of the specific miscibility of a solvent with polymeric beads.

In general, the basic requirement for a good solid support is its large surface area. The measurement of the surface area of the polymeric supports is thus one of the physical properties worth to study.

By nitrogen adsorption, the surface measurement was carried out for all the polymeric supports, except the one prepared in toluene (Table 4.10). The result clearly indicated that methylisobutyl carbinol was the most appropriate solvent for the preparation of the polymeric support since largest surface area and highest total pore volume were afforded.

Table 4.10 Surface measurement of polymeric supports in the variety of solvent type at 50 percent of total monomer mixture.

Solvent type	Specific surface area (m^2/g)	Total pore volume $(*10^{-2} \ cc/g)$
MIBC	6.23	2.11
ISO	3.48	1.18
BU	1.54	0.52
CY	2.48	0.84
CN	3.78	1.28
TO	no measure	no measure

Furthermore, the surface area and the total pore volume were also influenced by the amount of methylisobutyl carbinol. When the amount of methylisobutyl carbinol was 50% of the total amount of the monomer mixture, the highest values of both surface area and total pore volume were obtained comparing to the other proportions (Table 4.11). It was concluded that methylisobutyl carbinol acted as the best solvent for this polymeric support system.

Table 4.11   Surface measurement of polymeric supports in the
variety of methylisobutyl carbinol content

Percentage of MIBC in mono-mer mixture	Specific Surface area (m^2/g)	Total pore volume (cc/g)
40	5.97	2.08
50	6.23	2.11
60	5.99	2.01

4.2.3   Preparation of crosslinked polymers

As mentioned in the previous section that 50%
methylisobutyl carbinol was the most suitable for preparing a
good polymeric support with 10% DVB, different percent crosslinks
were also attempted under the same condition.   Polymerization was
thus carried out with 3, 10 and 20% DVB as shown below.
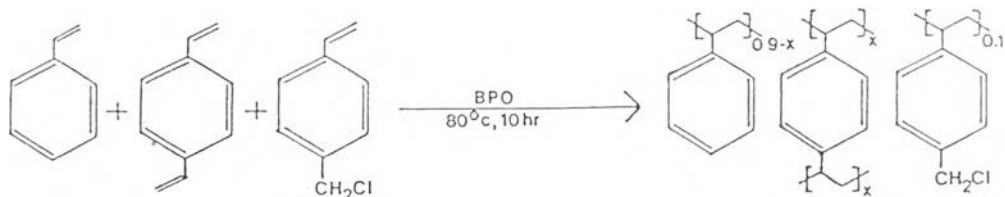
Let x = 0.03 ; PX–3

x = 0.10 ; PX–10

x = 0.20 ; PX–20

Scheme 4.7

Table 4.12 The elemental analysis of poly(styrene-co-divinyl benzene-co-vinylbenzyl chloride).

Polymeric support	yield (%)	Percent of elemental				T_g (^{O}C)
		C^a	H^a	Cl		
				calcd[a]	found[b]	
PX-3	90.2	89.13	7.62	3.25	2.15	125
PX-10	90.6	89.60	7.23	3.17	2.15	135
PX-20	90.7	88.94	7.91	3.15	2.14	150

[a] by elemental analyser, the subtraction of C,H from 100% gave %Cl
[b] by modified volhard method

From the elemental analysis for carbon and hydrogen (Table 4.12), the chloride content of polymeric supports could be calculated. The results were similar for all three different percent crosslinks. Although the monomer feed ratios of styrene and divinyl benzene were varied, both monomers had very similar structure. It was thus assumed that they had the similar monomer reactivity ratio. However, the chloride contents determined by modified volhard method were different from the calculation, resulted from the elemental analysis. This could be explained that by modified volhard method, the probability of pyridine

to react with chlorine atom might be limited dependent on the pore size. In case of the very small pore size, pyridine could penetrate into the pore only when the pressure outside was higher than the capillary force inside the pore. It was thus possible that chlorine atom embeded inside the very small pore could not be digested. Although the longer time of the digestion with pyridine was conducted, the results were not significantly different, indicating that all digested chlorine was obtained. By elemental analysis, the sample was heated at very high temperature leading to decomposition point. Therefore, all chlorine atom in the sample could be determined.
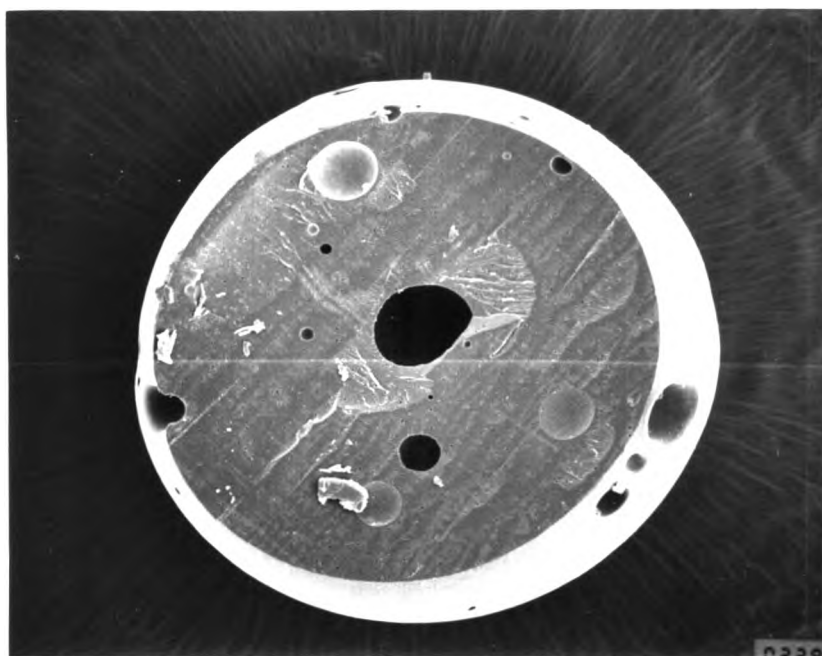

Figure 4.10 Scanning electron micrograph of x-section of
poly(styrene-co-divinyl benzene -co-
vinylbenzyl chloride) with 10 % DVB,
methylisobutyl carbinol used as solvent,
magnification with 100 times.

In comparison, surface measurement showed that the polymeric support with 20% DVB had the highest specific surface area, 21.79 m^2/g, and the highest total pore volume, 5.88 cc/g (Table 4.13). With the same weight of polymeric beads, less percent of crosslinking should give the larger pore size, in other words less number of pores. Therefore polymeric beads with 3% DVB gave less specific surface area and smaller total pore volume than 10 and 20% DVB, respectively.

Table 4.13   Surface measurement of polymeric supports in the variety of DVB content.

Percentage of divinyl benzene	Specific surface area (m^2/g)	Total pore volume (cc/g)
3	4.12	1.65
10	6.23	2.11
20	21.79	5.88

From the scanning electron micrographs (Figure 4.10) of poly(styrene-co-divinyl benzene-co-vinylbenzyl chloride) with 10 % DVB, methylisobutyl carbinol used as solvent , it was shown that the formation of void occurred also (Figure 4.11 (a), (b)). It was noticed that the void distribution in the bead was not regular and the size varied as well.

(a) 35 times
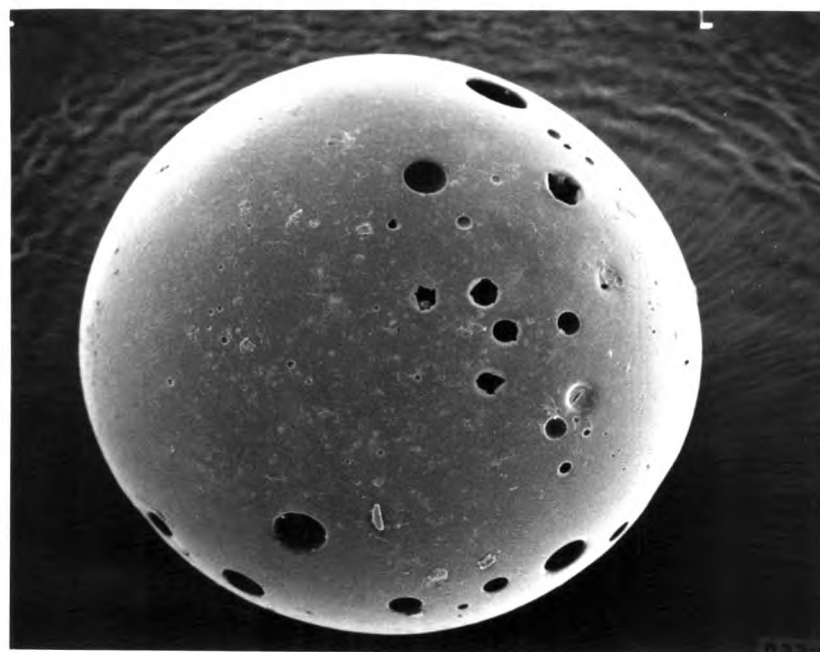
(b) 100 times

Figure 4.11   Scanning electron micrographs of poly(styrene-co-
              divinyl benzene-co-vinylbenzyl chloride) with
              10% DVB, methylisobutyl carbinol used as solvent,
              magnification with :(a) 35 times, (b) 100 times

The bead formation could probably occurred as layer by layer and during this time the void could possibly be constructed. This phenomenon clearly revealed by the scanning electron micrograph (Figure 4.12).
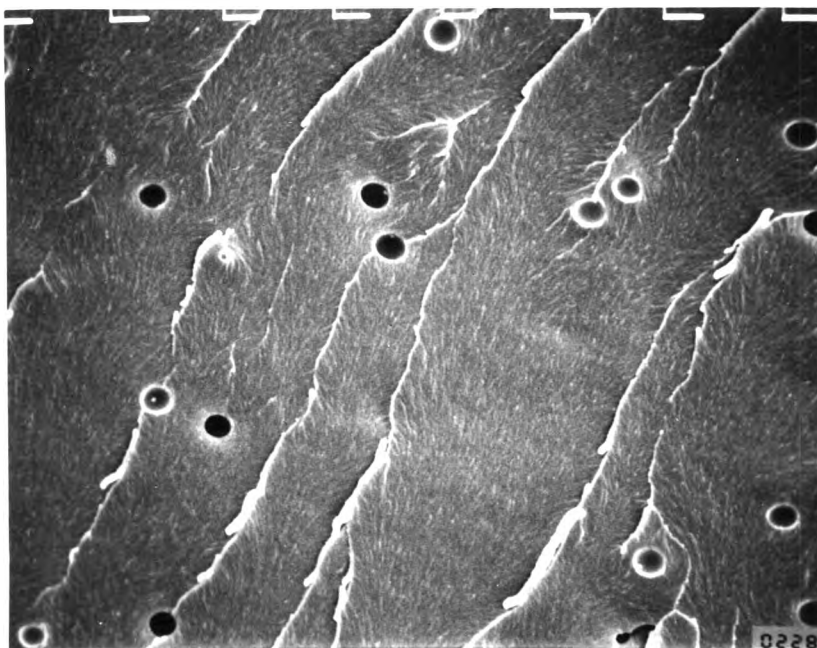
Figure 4.12 Scanning electron micrograph of x-section of poly(styrene-co-divinyl benzene-co-vinylbenzyl chloride) with 10% DVB, methylisobutyl carbinol used as solvent, magnification with 1500 times.

The differential scanning calorimetry output of poly (styrene-co-divinyl benzene-co-vinylbenzyl chloride) (Figure 4.13) showed that the melting temperature of the polymer with 3, 10 and 20% DVB were 411.16 ^{O}C, 420.54 ^{O}C and 428.13 ^{O}C, respectively. These values related with the rigidity and mobility of the polymeric chains. The more percent of DVB
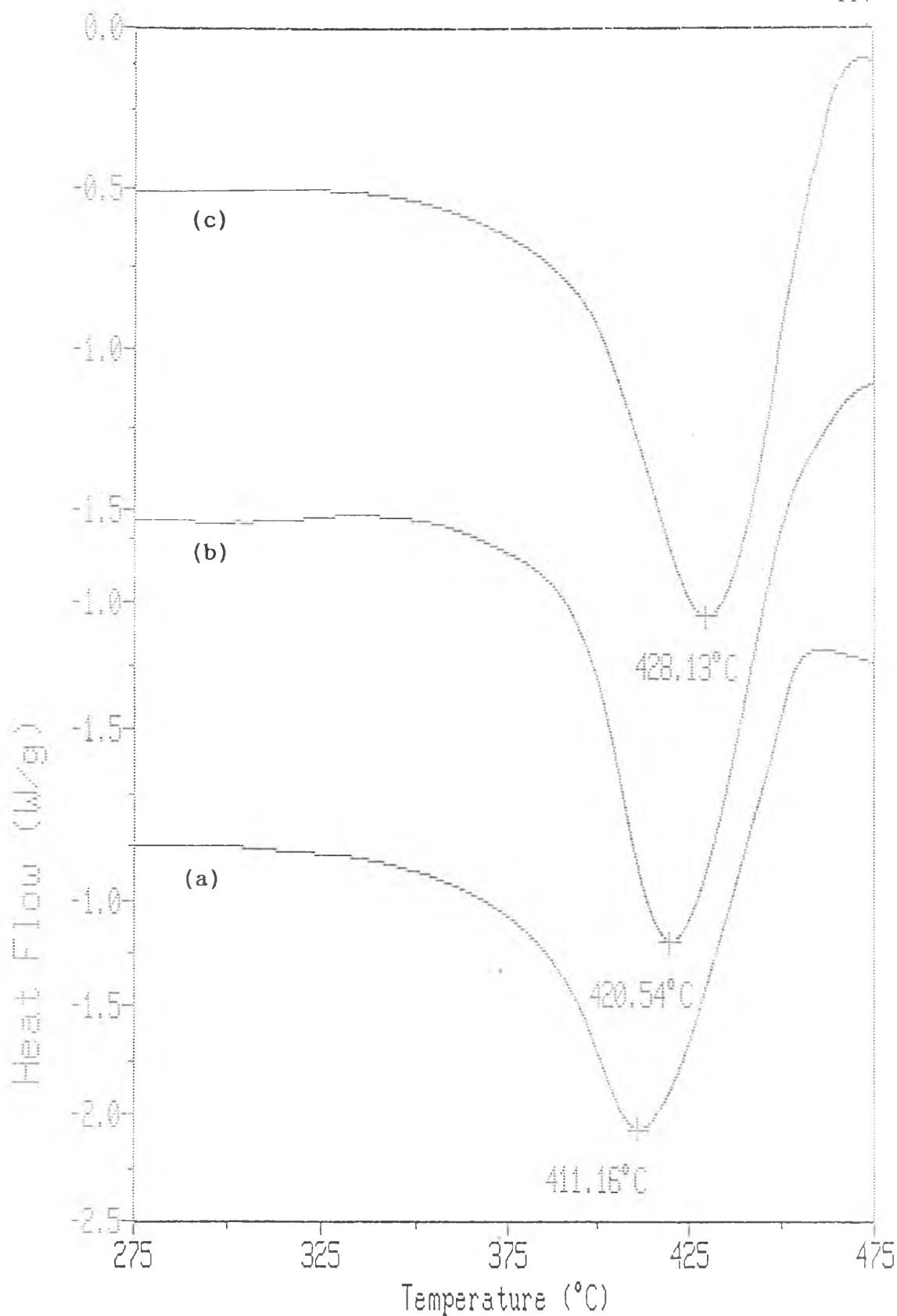
Figure 4.13 The differential scanning calorimetry output of
poly(styrene-co-divinyl benzene-co-vinylbenzyl
chloride) (a) PX-3. (b) PX-10 and (c) PX-20

present, the more rigidity and the more difficult mobility of the polymeric chains would be. It could be summarized that the percent crosslink could be selected to suit the temperature of each application.

4.3 Anchoring anthranillic acid to poly(styrene-co-divinyl benzene-co-vinylbenzyl chloride

In order to anthranilic acid serves as a bidentate ligand, which can bind the metal through the amino and carboxyl groups. Anchoring anthranilic acid to poly(styrene-co-divinyl benzene-co-vinylbenzyl chloride) accomplished through the reaction sequence shown in following equation.

Scheme 4.8
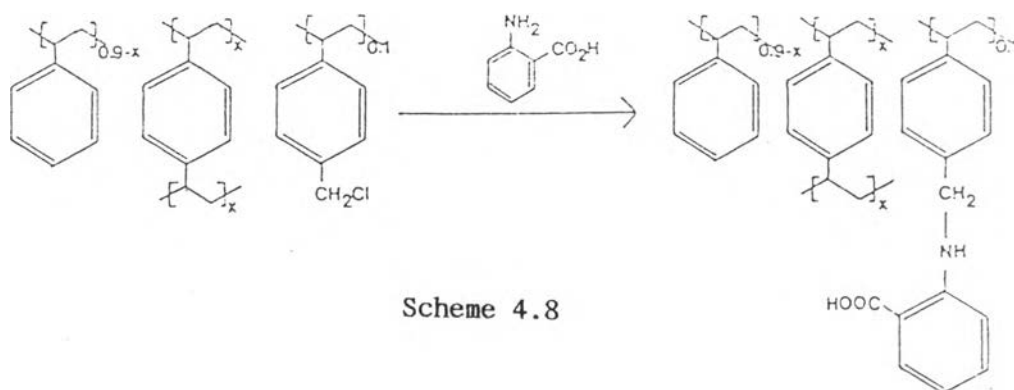
Let x = 0.03 ; PL-3

x = 0.10 ; PL-10

x = 0.20 ; PL-20

The elemental analysis of poly(styrene-co-divinyl benzene -co-vinylbenzyl chloride) anchoring anthranilic acid was shown in Table 4.14. The glass transition temperature(T_g) of polymeric

PS-3

PL-3

PS-10

PL-10

PS-20

PL-20
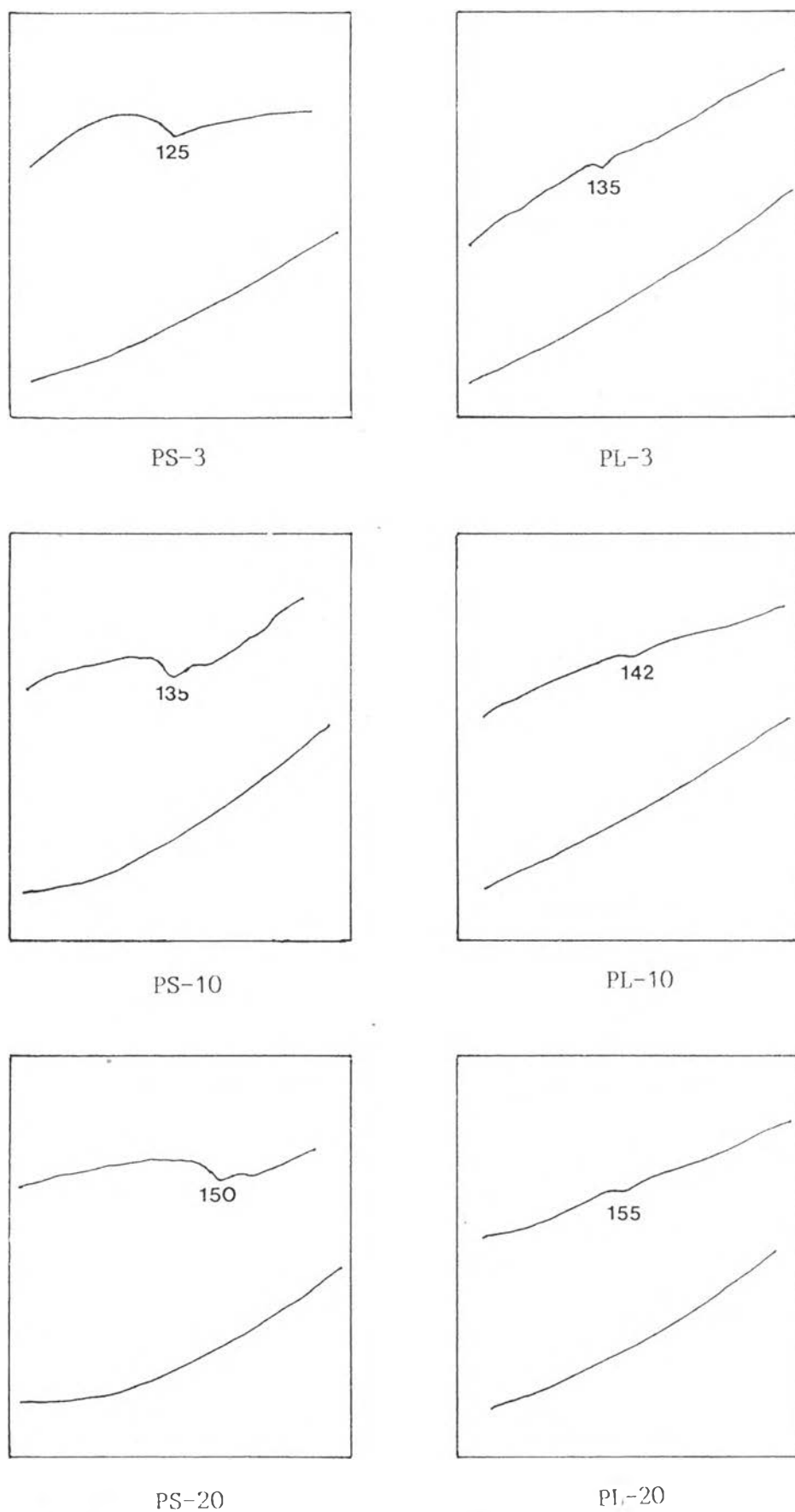
Figure 4.14 The differential thermograms of polymeric supports and
polymeric ligands

supports and polymeric ligands with 3. 10 amd 20% DVB were measured by differential thermal analyzer (Figure 4.14).

Table **4.14**   The elemental analysis of poly(styrene-co-divinyl benzene-co-vinyl benzyl chloride) anchoring anthranilic acid.

Polymeric ligand	Percent of elemental			T_g (^{O}C)
	C	H	N	
PL-3	89.08	7.75	0.56	135
PL-10	89.24	7.72	0.54	142
PL-20	88.59	7.73	0.54	155

There were the lines of evidence favoring nitrogen alkylation that benzyl chloride and anthranilic acid yield the N-alkylated product. The typical FT-IR spectrum (Figure 4.15) of the polymeric ligand revealed the carbonyl absorption at 1695 cm^{-1} to be more in accordance with a hydrogen bonding carboxylic acid than an ester. Other assignments were concluded in Table 4.15.
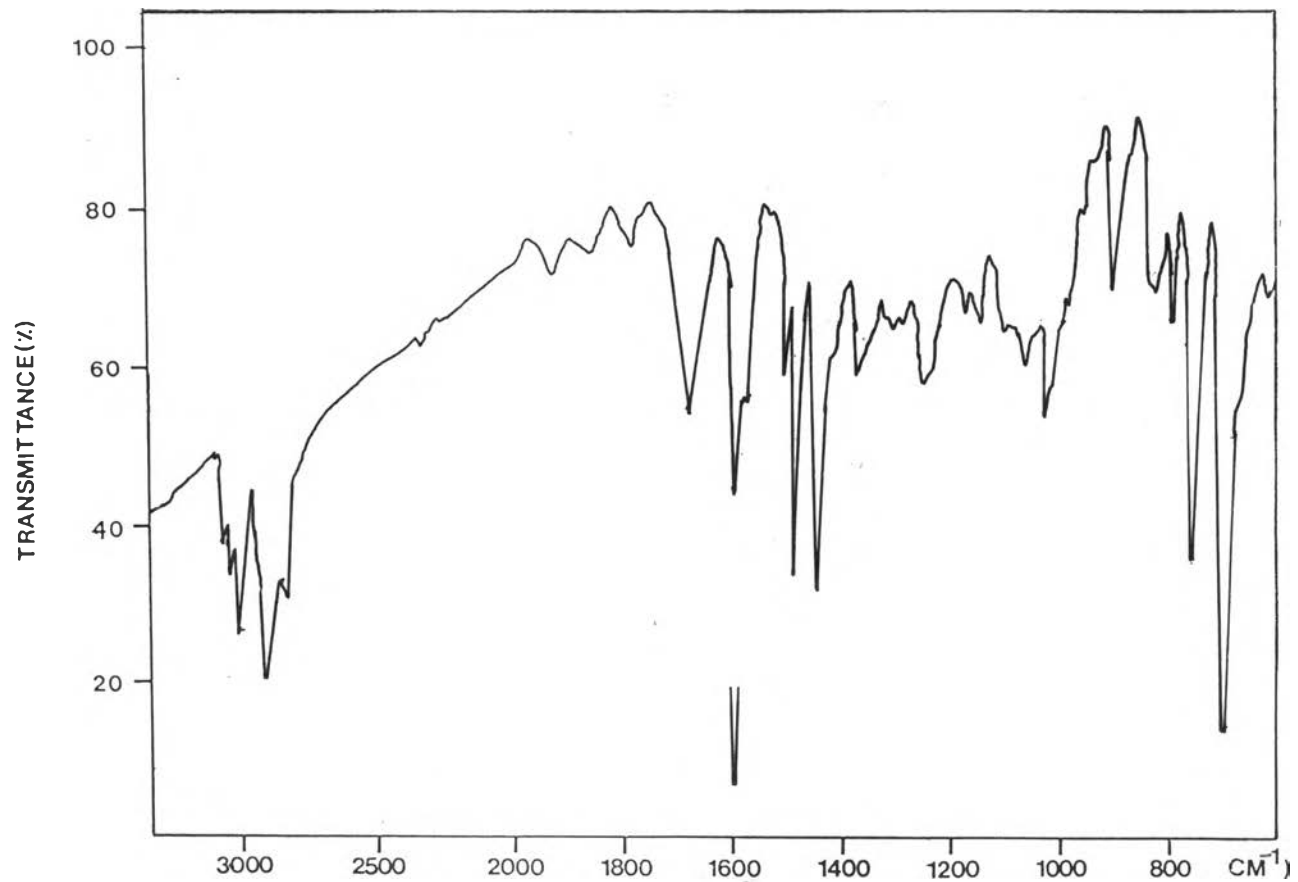
Figure 4.15 The typical FT-IR spectrum (KBr) of poly(styrene-co-divinyl benzene-co-vinylbenzyl chloride) with 10% DVB anchoring anthranilic acid

Table 4.15 The assignment for the typical FT-IR spectrum of

poly(styrene-co-divinyl benzene-co-vinyl

benzyl chloride) anchoring anthranilic acid.

Absorption frequency (cm^{-1})	Tentative assignment of 10% of DVB
3024	C-H aromatic str.
2920	C-H aliphatic str.
1695	C=O str.
1601,1492,1450	C=C aromatic str.
699	C-Cl str.

Accordingly, the percent of nitrogen content was measured by the elemental analyser. The nitrogen content also related with anthranilic acid ligand in polymeric ligand. So, the convenient method was modified volhard method and its detail was revealed in appendix I. The variable parameters i.e. solvent type, time and temperature were studied as follows.

The reaction between polymeric supports with 3, 10 and 20% DVB and anthranilic acid ligand were tested for 24 hours at room temperature in dried and non-dried solvents, results being

<u>Table 4.16</u> Effect of solvent type on the reaction between the polymeric supports and anthranilic acid.

Run No.	Solvent type	Temperature (^{o}C)	Time (hr)	Percent of DVB					
				3		10		20	
				%Cl[b]	%Cl[c]	%Cl[b]	%Cl[c]	%Cl[b]	%Cl[c]
1	acetone[a]	RT	24	2.15	2.04	2.15	2.04	2.14	2.05
2	acetone	RT	24	2.15	2.04	2.15	2.05	2.14	2.06
3	DMF[a]	RT	24	2.15	2.00	2.15	2.00	2.14	1.99
4	DMF	RT	24	2.15	2.00	2.15	2.00	2.14	1.99
5	ether[a]	RT	24	2.15	2.03	2.15	2.03	2.14	2.02
6	ether	RT	24	2.15	2.03	2.15	2.04	2.14	2.03

a   solvent was dried.

b   before binding

c   after binding

shown in Table 4.16 and   the percent of chloride   content replaced with   ligand (%Cl[b] minus %Cl[c]) was shown as   bar   chart in Figure 4.16. The percent of chloride content of polymeric supports with 3, 10 and 20% DVB were about 2.15, 2.15 and 2.14, respectively. After the polymeric supports were anchored with anthranilic acid, the polymeric ligand with different percent of

DVB, using dried solvents and non-dried solvents, would give the similar results. It was noticed that dimethyl formamide gave the best result. So, the solvent chosen as the slurrying solvent in anchoring ligand with polymeric supports was non-dried dimethyl formamide.

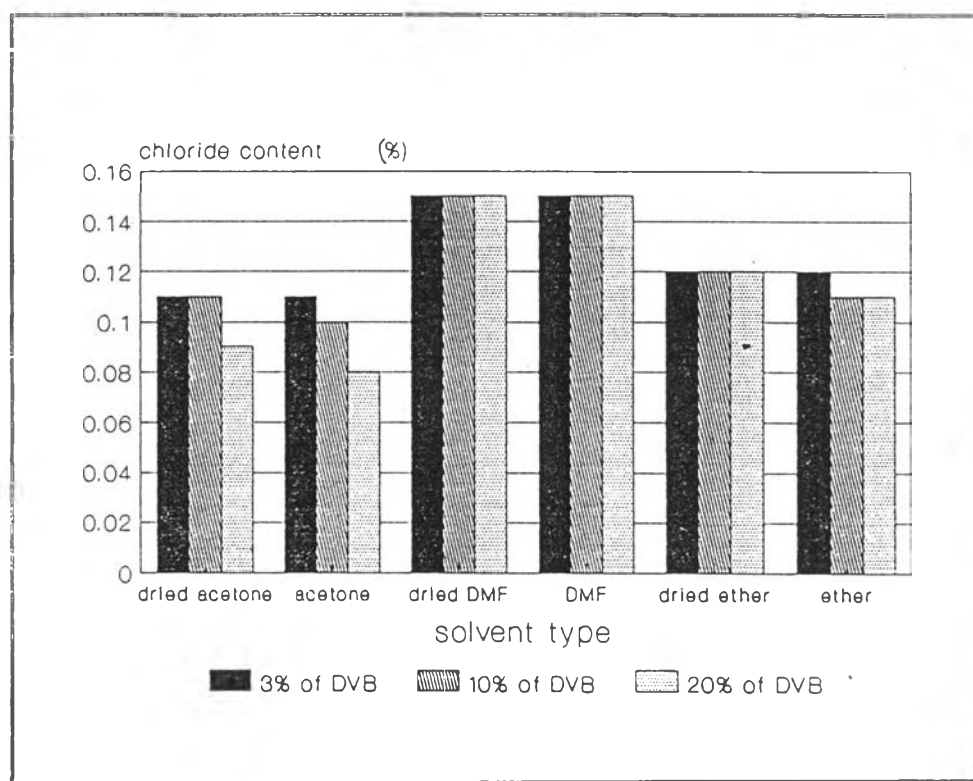Figure 4.16 Effect of solvent type on the percent of chloride content replaced with anthranilic acid

Effect of the time on the reaction between the polymeric supports and anthranilic acid ligand at room temperature and non-dried dimethyl formamide as a solvent were shown in Table 4.17 and the percent of chloride content replaced with ligand (%Cl[a] minus %Cl[b]) was shown as bar chart in Figure 4.17. When

When the time was consumed until the anchoring process was not changed. Finally, the optimum time was corresponded to 22 hours.

Table 4.17 Effect of time on the reaction between the polymeric supports and anthranilic acid.

Run No.	Solvent type	Temperature (^{O}C)	Time (hr)	Percent of DVB					
				3		10		20	
				$\%Cl^a$	$\%Cl^b$	$\%Cl^a$	$\%Cl^b$	$\%Cl^a$	$\%Cl^b$
1	DMF	RT	18	2.15	2.03	2.15	2.03	2.14	2.04
2	DMF	RT	20	2.15	2.01	2.15	2.03	2.14	2.04
3	DMF	RT	22	2.15	2.00	2.15	2.00	2.14	1.99
4	DMF	RT·	24	2.15	2.00	2.15	2.00	2.14	1.99
5	DMF	RT	26	2.15	2.00	2.15	2.00	2.14	1.99

a   before binding

b   after binding
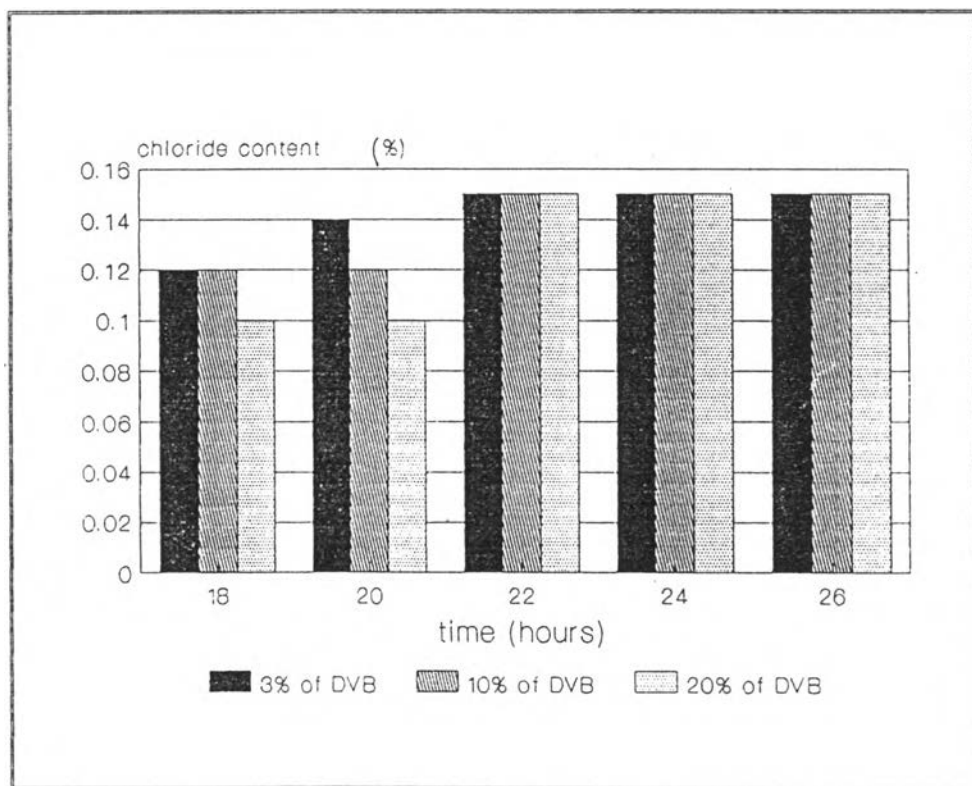
Figure 4.17   Effect of time on the percent of chloride
              content replaced with anthranilic acid

The   reaction between the polymeric supports and anthranilic

acid ligand for 22 hours and non-dried dimehtyl formamide as a

solvent was studied at the different temperatures and the results

were shown in Table 4.18. The percent of chloride content

replaced with ligand (%Cl^a minus %Cl^b) was shown as bar chart in

Figure 4.18. When the reaction was heated, the chloride content

of the polymeric ligands in three different crosslinks was

constant at the optimum temperature of 90°C.

124

Table 4.18 Effect of temperature on the reaction between the
polymeric supports and anthranilic acid.

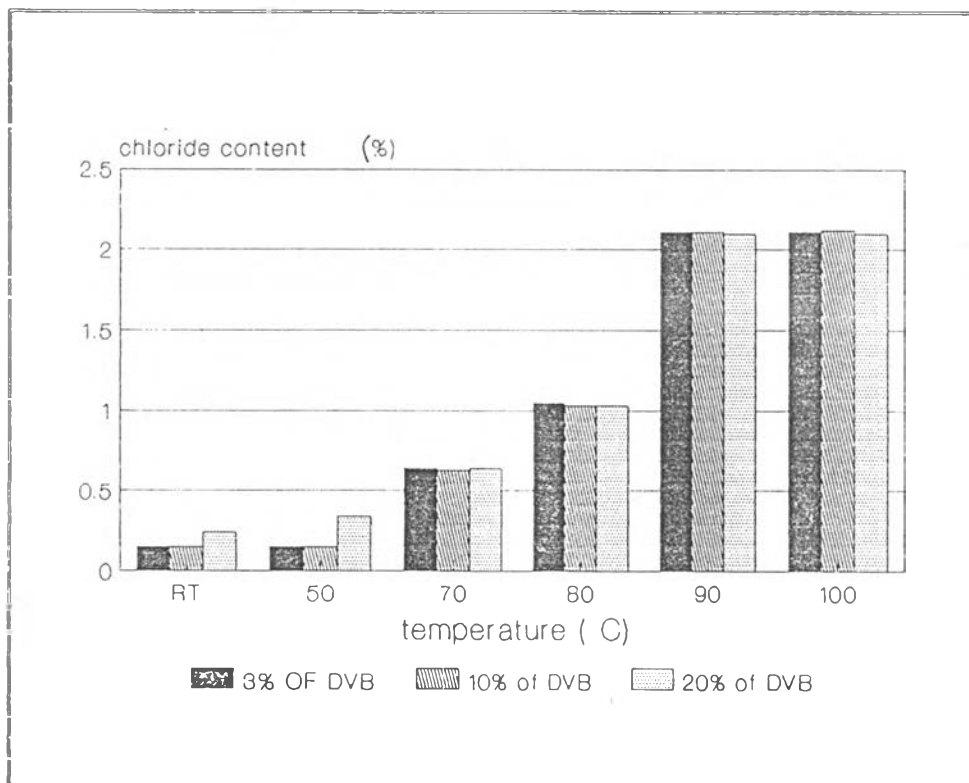| Run No. | Solvent type | Temperature (^{O}C) | Time (hr) | Percentages of DVB | | | | | |
				3		10		20	
				%Cl^a	%Cl^b	%Cl^a	%Cl^b	%Cl^a	%Cl^b
1	DMF	RT	22	2.15	2.00	2.15	2.00	2.14	1.90
2	DMF	50	22	2.15	2.00	2.15	2.00	2.14	1.80
3	DMF	70	22	2.15	1.51	2.15	1.52	2.14	1.50
4	DMF	80	22	2.15	1.10	2.15	1.12	2.14	1.11
5	DMF	90	22	2.15	0.04	2.15	0.04	2.14	0.04
6	DMF	100	22	2.15	0.04	2.15	0.03	2.14	0.04

a before binding

b after binding

Figure 4.18 Effect of temperature on the percent of chloride
content replaced with anthranilic acid

Finally, the reaction between the polymeric supports and
anthranilic acid ligand should be summarized that polymeric
beads should be swelled in non-dried dimethyl formamide for
22 hours at the temperature of $90^{\circ}C$.

4.4 Complexation and reduction of poly(styrene-divinyl benzene-vinylbenzyl chloride) anchoring anthranillic acid and rhodium(III) chloride

The complex formation of poly(styrene-co-divinyl benzene-co-vinylbenzyl chloride) anchoring anthranilic acid in each crosslinks with rhodium trichloride was obtained Rh(III) polymer-bound catalysts. After the reduction reaction by sodium borohydride, the Rh(I) polymer-bound catalysts was synthesized as equation as below.
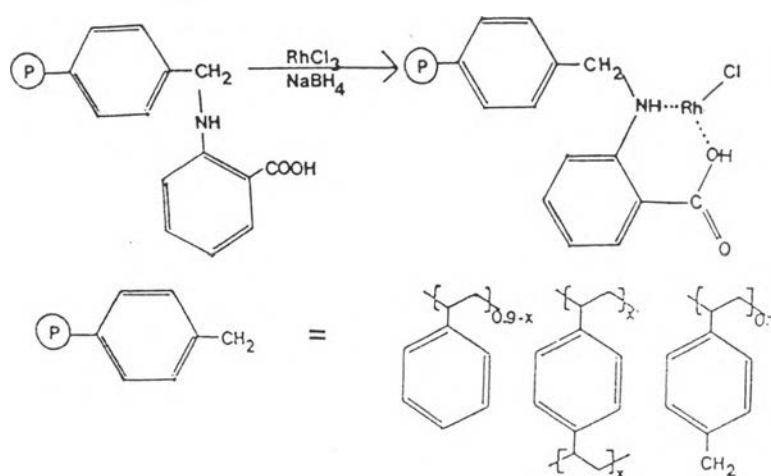
Let x = 0.03 ; PC-3

x = 0.10 ; PC-10

x = 0.20 ; PC-20

Scheme 4.9

The rhodium metal was attached to the polymeric ligands by suspending them in a small volume of basic sodium ethoxide solution. When the polymeric products were brought to the

vacuum oven in order to let the small pores inside the polymeric ligands react with the rhodium trichloride. It was observed that the yellowish reactants became red-brown products. And then the polymeric ligands with covalently binding Rh(III) chloride were treated with sodium borohydride and the Rh(I) polymer-bound catalyst was obtained. The colour of the product was black-brown.

Table 4.19   The elemental analysis of

Rh(I)polymer-bound catalysts

Polymeric Catalysts	Percent of elemental		
	C	H	N
PC-3	88.13	7.56	0.47
PC-10	88.32	7.64	0.45
PC-20	88.78	7.75	0.40

From the elemental analysis as shown in Table 4.19, it was confirmed that the anthranilic acid ligand still bound with the polymeric beads in each different crosslinks. In order to determine the rhodium content in polymeric catalysts, inductively coupled plasma techniques was carried out. The standard
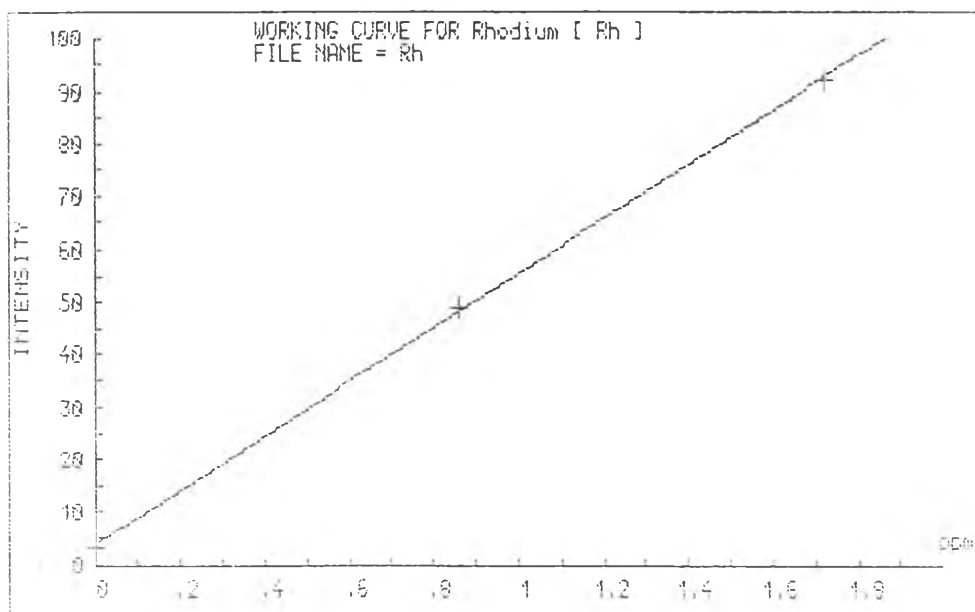
Figure 4.19   Standard calibration curve of the determination

of rhodium

Table 4.20   The   rhodium content in the polymeric catalysts.

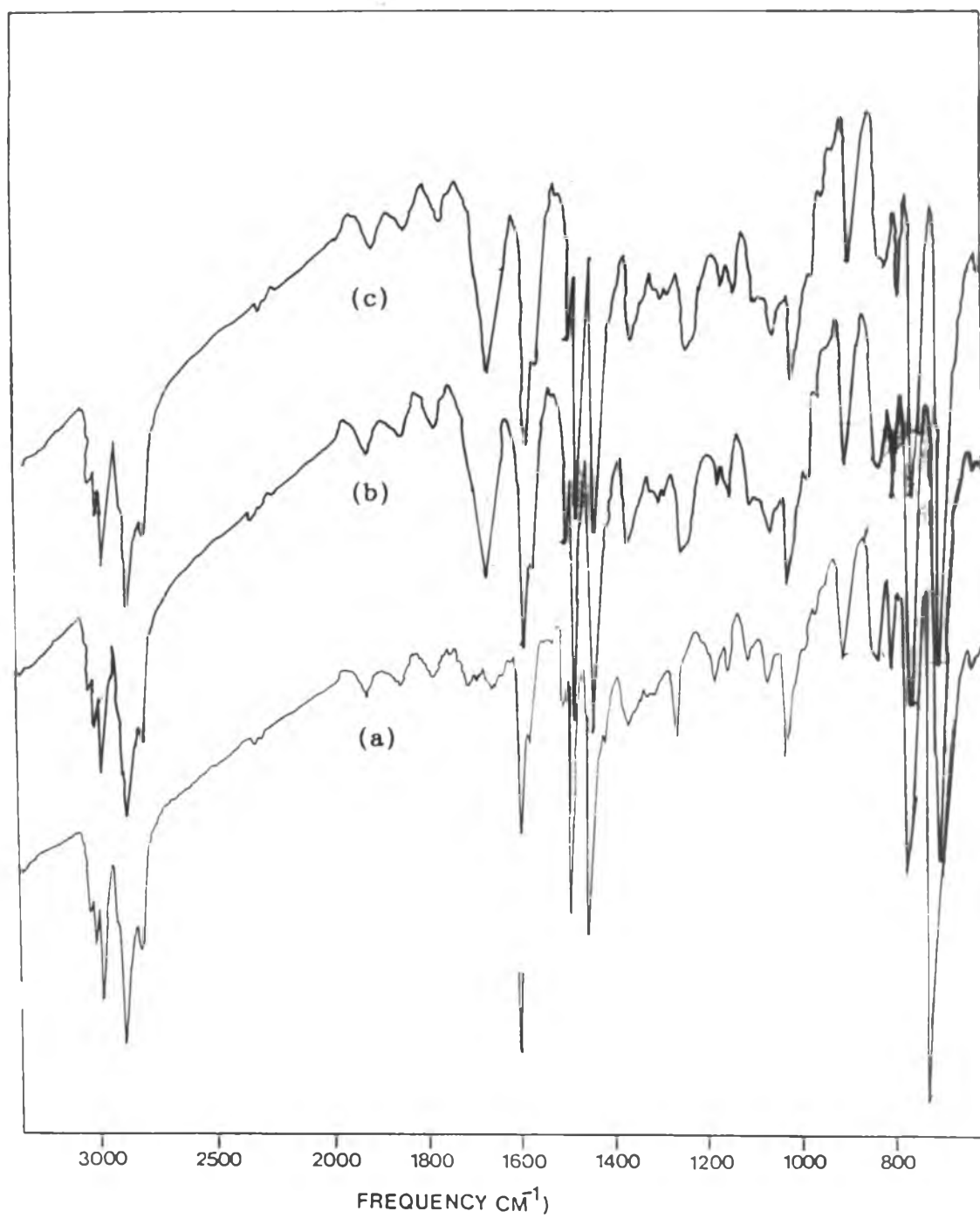| Polymeric catalysts	Rhodium content (mequiv/g of polymer)
PC-3	0.2095
PC-10	0.1662
PC-20	0.1498

Figure 4.20 The typical FT-IR spectra (KBr) of (a) PX-10,
(b) PL-10 and (c) PC-10

calibration curve of rhodium was plotted as shown in Figure 4.19.

From the data in Table 4.20 and elemental analysis data, they were summarized that rhodium(I) polymer-bound catalysts with 3, 10 and 20% DVB were synthesized. Accordingly, the typical FT-IR spectra (Figure 4.20) of polymeric supports, polymeric ligands and polymeric catalysts with 10% DVB were shown that at 1267 cm^{-1} of the spectra (b) which indicated that anthranilic acid was bound to the polymeric supports.

4.5 Preliminary study of catalytic cyclohexene hydrogenation using Rhodium(I) polymer-bound catalysts

Rhodium(I) polymer-bound catalysts
H$_2$(60 psig), room temperature

Scheme 4.11

When the polymeric catalysts were employed in hydrogenation the color irreversibly darkened. The hydrogenation of cyclohexene was largely dependent on bead swelling and the role of solvation during the course of hydrogenation. Bead swelling was highly visible and important in the catalytic process because hydrogenation was considered to occur within the polymeric beads.

From the preliminary study of cyclohexene hydrogenation. it was revealed that Rh(I) polymer-bound catalysts with 3, 10 and 20% DVB could hydrogenate cyclohexene at room temperature by fixing rhodium content in each catalyst. The mixture was drawn out of the bomb reactor at the certain interval of time in order to determine the cyclohexane product by gas chromatography (Table 4.21 and Table 4.22).

Table 4.21 The peak area of cyclohexene chromatogram from cyclohexene hydrogenation using Rh(I) polymer-bound catalysts.

Fraction no.	Time (min)	Peak Area		
		3% of DVB	10% of DVB	20% of DVB
1	0	268400	276450	280145
2	60	257881	266045	270544
3	90	257030	265332	270118
4	120	255631	263867	269748
5	150	248500	257880	265439
6	180	237540	249295	264679
7	210	221131	236531	241108
8	240	215734	225144	239756

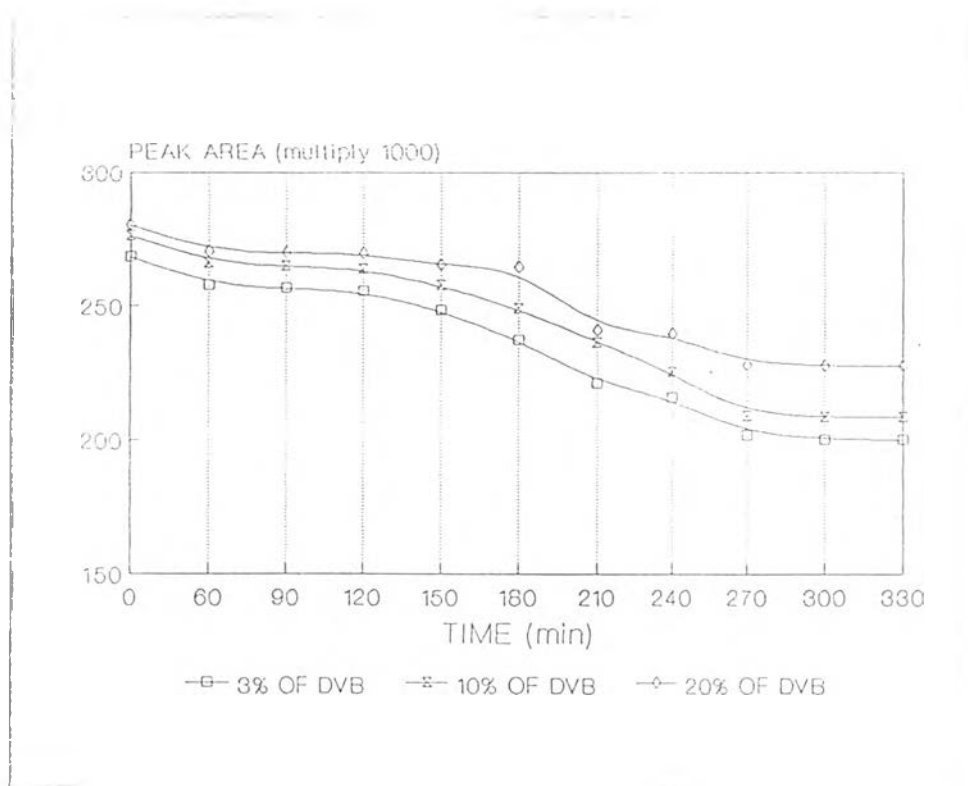| Fraction no.	Time (min)	Peak Area		
		3% of DVB	10% of DVB	20% of DVB
9	270	201834	208829	227874
10	300	200234	208656	227616
11	330	200143	208651	227560

Figure 4.21 The conversion of cyclohexene hydrogenation by Rh(I)
polymer-bound catalyst with 3, 10 and 20% DVB

Table 4.22 The peak area of cyclohexane chromatogram from
cyclohexene hydrogenation using Rh(I)
polymer-bound catalysts.

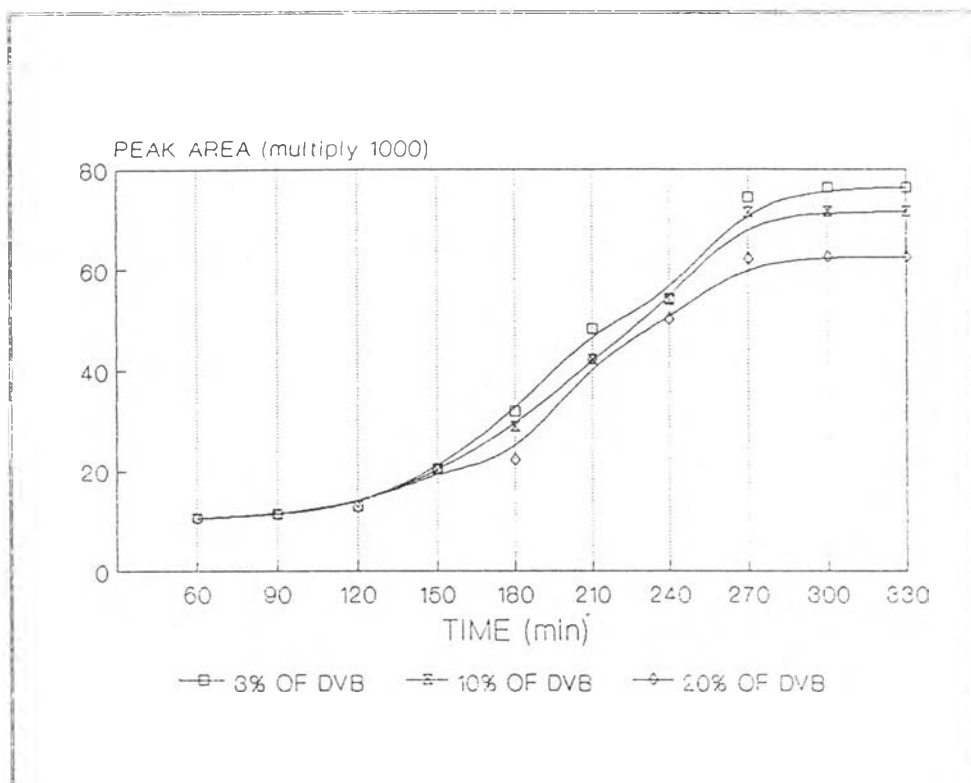| Fraction no.	Time (min)	Peak Area		
		3% of DVB	10% of DVB	20% of DVB
1	60	10540	10410	10400
2	90	11420	11121	11105
3	120	12850	12745	12641
4	150	20515	20013	20023
5	180	31775	28818	22189
6	210	48250	42018	42005
7	240	54380	54002	50105
8	270	74311	71311	62226
9	300	76216	71484	62495
10	330	76311	71494	62582

PEAK AREA (multiply 1000)

Figure 4.22 The conversion of cyclohexane hydrogenation by Rh(I) polymer-bound catalyst with 3, 10 and 20% DVB

From the data using the polymeric catalyst with 3% DVB, it was found that the cyclohexane product increased with time upto five hours where the reaction became completed. On the condition that polymeric catalyst with 3% DVB which obtained polymeric catalyst with relatively big pore size to 10 and 20% DVB. However, it had the relatively least surface area to the others.

Considering the polymeric catalyst with 10% DVB, it showed the similar conversion curve. However, the cyclohexane conversion was relatively lower than the polymeric catalyst with 3% DVB. It could be explained that the reaction could be continued in correspondent with the pore size of the polymeric catalysts.

When the surface area was discussed in hydrogenation conversion of polymeric catalysts with the different percent of DVB, it was revealed that the polymeric catalysts with 20% DVB which has the highest surface area, gave the poor result with respect to 3 and 10% DVB, though it has the highest surface area. This might be considered that the rhodium catalyst was embeded inside the polymeric beads, thus the conversion of cyclohexane hydrogenation depends especially on the polymer pore size.

Two mechanisms could most reasonably contribute to this loss of activity. One, the sloughing of the polymer was well known for polystyrene. Since the metal appeared to be concentrated at or near the surface of the bead, a low degree of sloughing could alter catalyst activity substantially. Two, the rearrangement of the ligands might occur.

Table 4.23 The rhodium leaching content from the
          polymeric catalysts

Polymeric catalysts	Rhodium leaching content (mequiv/g of polymer)
PC-3	0.045
PC-10	0.038
PC-20	0.035

The leaching of rhodium content from the polymeric support
was determined after hydrogenation. This was performed by the
analysis of rhodium content in the catalysts recovered from the
reaction using ICP techniques. The substraction from the rhodium
content in the polymeric catalysts before subjective to
hydrogenatation gave rhodium leaching content as shown in
Table 4.23. It was found that for the polymeric catalysts with
3% DVB the rhodium was leached from the polymeric support
in the highest content (21.48%). It could be explained that the
catalyst with big pore size, the metal could be highly
effected by various factors such as the hydrogen pressure,
therefore, the possibility of metal leaching should be higher
than in the case of catalyst with small pore size. The catalysed
hydrogenation of cyclohexene readily reacted at room temperature.
The introduction of molecular hydrogen into unsaturated bonds

could be proposed as follows:

1. Dissociation of one of the ligands.

2. Hydrogen activation by coordination
   (oxidative addition of hydrogen).

3. Substrate activation by coordination.

4. Hydrogen transfer to the substrate.

5. Liberation of the hydrogenated product
   and catalyst regeneration.

These steps in hydrogenation of cyclohexene could be expressed by the following Scheme, where stereochemistry of the ligands was neglected: the dihydride complex formation by oxidative addition was followed by cyclohexene coordination. Insertion of the coordinated cyclohexene to the rhodium-hydrogen bond gave the cyclohexylrhodium complex. Finally, cyclohexanes were liberated by the coupling of the cyclohexyl group and hydrogen attached to the same rhodium with regeneration of the complex.

Scheme 4.12